iScience

CellPress
OPEN ACCESS

Article

Breast cancer therapies reduce risk of Alzheimer's disease and promote estrogenic pathways and action in brain

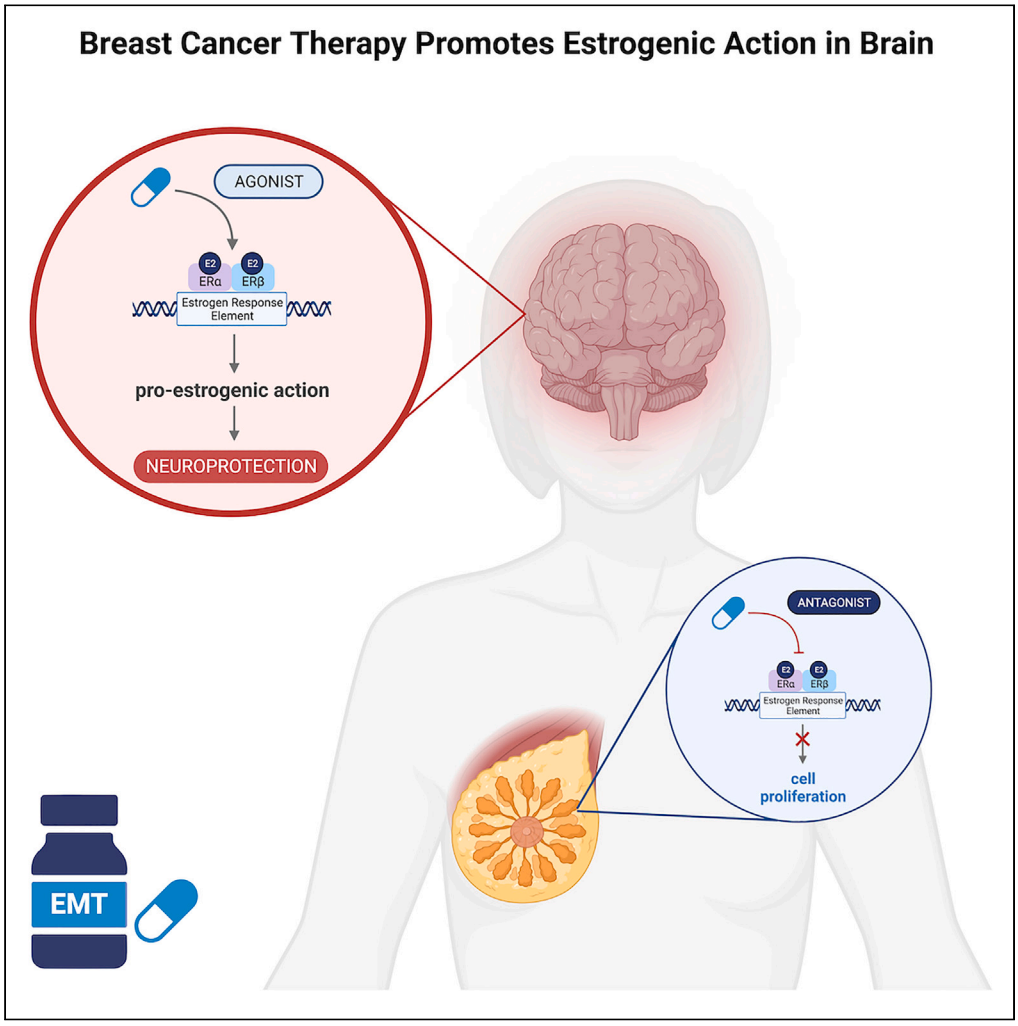

Gregory L. Branigan, Georgina Torrandell-Haro, Shuhua Chen, ..., Helena Cortes-Flores, Francesca Vitali, Roberta Diaz Brinton

rbrinton@arizona.edu

Highlights

We conducted reverse translational analyses to determine impact of EMTs on AD risk

EMT exposure was associated with reduced risk of AD in women with breast cancer

Mechanistic data indicate that select EMTs function as estrogenic agonist in brain

Branigan et al., iScience *26*, 108316
November 17, 2023
https://doi.org/10.1016/j.isci.2023.108316

iScience

CellPress
OPEN ACCESS

Article

Breast cancer therapies reduce risk of Alzheimer's disease and promote estrogenic pathways and action in brain

Gregory L. Branigan,[1,2,4] Georgina Torrandell-Haro,[1,2] Shuhua Chen,[1] Yuan Shang,[1] Samantha Perez-Miller,[1] Zisu Mao,[1] Marco Padilla-Rodriguez,[1] Helena Cortes-Flores,[1] Francesca Vitali,[1,5] and Roberta Diaz Brinton[1,2,3,6,*]

SUMMARY

Worldwide, an ever-increasing number of women are prescribed estrogen-modulating therapies (EMTs) for the treatment of breast cancer. In parallel, aging of the global population of women will contribute to risk of both breast cancer and Alzheimer's disease. To address the impact of anti-estrogen therapies on risk of Alzheimer's and neural function, we conducted medical informatic and molecular pharmacology analyses to determine the impact of EMTs on risk of Alzheimer's followed by determination of EMT estrogenic mechanisms of action in neurons. Collectively, these data provide both clinical and mechanistic data indicating that select EMTs exert estrogenic agonist action in neural tissue that are associated with reduced risk of Alzheimer's disease while simultaneously acting as effective estrogen receptor antagonists in breast.

INTRODUCTION

Incidence of breast cancer accounted for almost one-third of all female cancers in 2021 and is projected to increase in parallel with global population.[1,2] In 2022 alone, over 287,850 new cases of breast cancer were diagnosed representing 15.2% of all new cases of cancer.[1] Approximately 1 in 8 or 12.8% of women will be diagnosed with breast cancer during their lifetime.[2] As of 2016, 3,477,866 women were estimated to be living with breast cancer in the United States.[3] The success in survival rate following breast cancer is accompanied by long-term use of therapeutics that target estrogen action.

As a result of the high prevalence of estrogen-positive breast cancer,[2,3] there are multiple breast cancer therapies targeting the estrogen receptor or the production of estrogen herein referred to as estrogen-modulating therapies (EMTs). These therapeutics are orally delivered and have systemic distribution that includes brain which raises the question of their potential to impact neurological function and health. EMTs include the selective estrogen receptor modulators (SERMs; tamoxifen and raloxifene) and aromatase inhibitors (steroidal, exemestane; nonsteroidal, anastrozole and letrozole).[4] These drugs have been used for the treatment of estrogen receptor–positive breast cancers and have been shown to antagonize estrogen's effects at the level of the breast tissue[5] but are known to have tissue-specific effects.[6–10]

As the number of women diagnosed with breast cancer increases and survival rates improve, the number of women being treated with EMTs at risk for other diseases will escalate.[11,12] Given the increasingly strong evidence that decline in estrogen can be a risk factor for Alzheimer's disease (AD)[13–16] and the increasing incidence of breast cancer prompting EMT use, determining the implications of systemically delivered EMT treatment that could affect estrogen action in brain. Potential neurological risks and/or benefits of EMTs that reduce breast cancer recurrence will have increasing importance for long-term brain health.

We and others have conducted retrospective clinical analyses indicating that exposure to EMT for the treatment of breast cancer is paradoxically associated with a decreased risk of AD later in life.[17,18] The report herein replicates findings of the association between EMT and decreased AD risk in a dataset of over 300,000 and investigates mechanisms by which EMTs act on neurons. Outcomes of these reverse translation analyses provide insights into cellular and molecular mechanisms of EMTs including regulation of neuronal morphology, electrophysiology, mitochondrial bioenergetics and dynamics, and regulation of estrogenic transcriptional pathways.

[1]Center for Innovation in Brain Science, University of Arizona; Tucson AZ, USA
[2]Department of Pharmacology, University of Arizona College of Medicine; Tucson AZ, USA
[3]Department of Neurology, University of Arizona College of Medicine; Tucson AZ, USA
[4]Medical Scientist Training Program, University of Arizona College of Medicine; Tucson AZ, USA
[5]Center of Bioinformatics and Biostatistics, University of Arizona College of Medicine; Tucson AZ, USA
[6]Lead contact
*Correspondence: rbrinton@arizona.edu
https://doi.org/10.1016/j.isci.2023.108316

RESULTS

EMT exposure is associated with reduced risk of AD

Of the 725,160 breast cancer patients within the Mariner dataset, 339,926 met inclusion/exclusion criteria and claims enrollment period requirements for analysis (Figure 1A). An index date to survey for a diagnosis of AD was set one year after the diagnosis of breast cancer to rule out any diagnosis likely from direct effects caused by chemotherapy or other interventions administered immediately after diagnosis before the start of EMT. Patient groups were defined according to the therapeutic intervention used. Of the 260,232 patients who met propensity score matching enrollment in the study, 130,116 received EMT (mean [SD] age, 65.9 [2.1] years) whereas 130,116 individuals (mean [SD] age, 72.5 [2.4] years) were not treated with EMT (Figure 1A, Table S2). EMT was initiated on average (SD) 160 days (5.4 months) following diagnosis of breast cancer. The mean (IQR) filled prescription days was 1210(1020). The drugs defined as EMT, patient counts, and median adherence rate for each drug are reported in Table S1. Patient demographics and comorbidities for those treated with EMT and the control patients appear in Table S2. ICD and generic drug codes used in this analysis appear in Table S3.

EMT exposure across all types was associated with a significant decrease in the diagnosis of AD (Figure 1). After propensity score matching, exposure to EMT was associated with a decreased incidence of AD (RR: 0.85; 95% CI: 0.79–0.93, $p < 0.001$) compared to patients not exposed to EMTs. The number of patients needed to treat to reduce risk of AD was 722 in the adjusted population.

To address potential selectivity of EMT to impact risk of any neurological degenerative disease (NDD composite of Alzheimer's, non-AD dementia, multiple sclerosis, Parkinson's, and amyotrophic lateral sclerosis) or AD, analysis of incidence by therapeutic mechanism of action was conducted (Figure 1B). Patients receiving EMTs were divided into four groups based on therapeutic target: SERMs tamoxifen and raloxifene, nonsteroidal aromatase inhibitors, and a steroidal aromatase inhibitor. Tamoxifen use was associated with significantly reduced risk of AD (RR, 0.44; 95% CI 0.41–0.47; $p < 0.001$; Figure 1B). In contrast, raloxifene exposure, while also an SERM, was associated with an increased risk of AD (RR, 1.18; 95% CI 1.07–1.30; $p < 0.01$; Figure 1B). Both nonsteroidal aromatase inhibitors, anastrozole and letrozole (RR, 0.83; 95% CI 0.76–0.89; $p < 0.001$; Figure 1B), and the steroidal aromatase inhibitor exemestane (RR, 0.83; 95% CI 0.76–0.89; $p < 0.001$; Figure 1B) were associated with a reduced risk of AD. Thus, the reduced relative risk seen in the EMT-treated population is primarily driven by patients receiving tamoxifen or aromatase inhibitors (Figure 1B). The propensity score-matched population was then used to generate Kaplan-Meier survival curves for NDD-free survival for each NDD subtype to evaluate the rate and percentage of the population who developed each disease (Figure 1C). Changes in rate of disease incidence between patients receiving EMTs compared to those not receiving EMTs mirror the results seen in the chi-square analysis (Figure 1C) and survival curves for each of the individual EMT classes are validated in the survival curves (Figures 1D–1G).

Molecular docking of EMTs to estrogen receptor suggests interaction

Using the DrugBank database, a drug-protein target network was generated to visualize overlapping targets for each of the EMT classes (Figure 2A). EMTs (diamond symbols) and their first protein targets (red circles) are represented in the network. As expected, tamoxifen and raloxifene share the greatest number of protein targets; however, tamoxifen interacts with a larger network of non-overlapping targets than the other EMTs (Figure 2A) including ERα and ERβ. The aromatase inhibitors all share the same protein target, which is the aromatase enzyme, CYP19A1 (Figure 2A).

Following the drug-protein network analysis, an analysis using the SWISS-ADME database was conducted using the chemical structures of EMTs and active metabolites to determine predicted blood-brain barrier penetration (Figure 2B). The results demonstrate that, with the exception of raloxifene, estradiol and each of the EMTs were predicted to cross the blood-brain barrier and thus interact with and impact the brain. Of interest, tamoxifen is not predicted to readily cross but its active metabolite 4-OH tamoxifen as well as endoxifen are blood-brain barrier penetrant.

To address the potential sites of EMT action, we conducted molecular docking using Glide Extra Precision mode through the Schrödinger platform to determine potential interactions between EMTs and human ERα and ERβ (Figures 2C–2F).

The docking analyses confirmed that E2 itself can interact with both agonist and antagonist states of ERα and ERβ, with docking scores below −10 kcal/mol signifying strong predicted interactions (Figure 2D). Tamoxifen and raloxifene only docked to the antagonist-bound states of the ERα and ERβ as would be predicted based on their original development for the treatment of breast cancer through antagonism of estrogen receptors. These results are also consistent with the experimental structures of ERα with 4-hydroxy tamoxifen[20] (Figure 2*E*) and with raloxifene.[21] Results of the docking analysis indicated unexpected interactions between the aromatase class of drugs and estrogen receptors. Indeed, both anastrozole and exemestane are predicted to interact with ERα and ERβ with docking scores between −7 and −9 indicating moderate to strong predicted interactions. Of importance, the predicted interaction of exemestane with ERα as an agonist was greater whereas anastrozole was predicted to interact at approximately equal strength both agonist and antagonist conformations of both ERα and ERβ (Figures 2E and 2F).

In vivo EMT treatment promotes estrogen-related transcriptomic pathways in hippocampus

To model the interactions between EMTs and the brain, an *in vivo* set of experiments were conducted in which Sprague-Dawley rats were treated with either E2 or EMTs via intraperitoneal injection to determine impact on brain pathways. All treatment doses in the rat were allometrically scaled to represent human dosing.

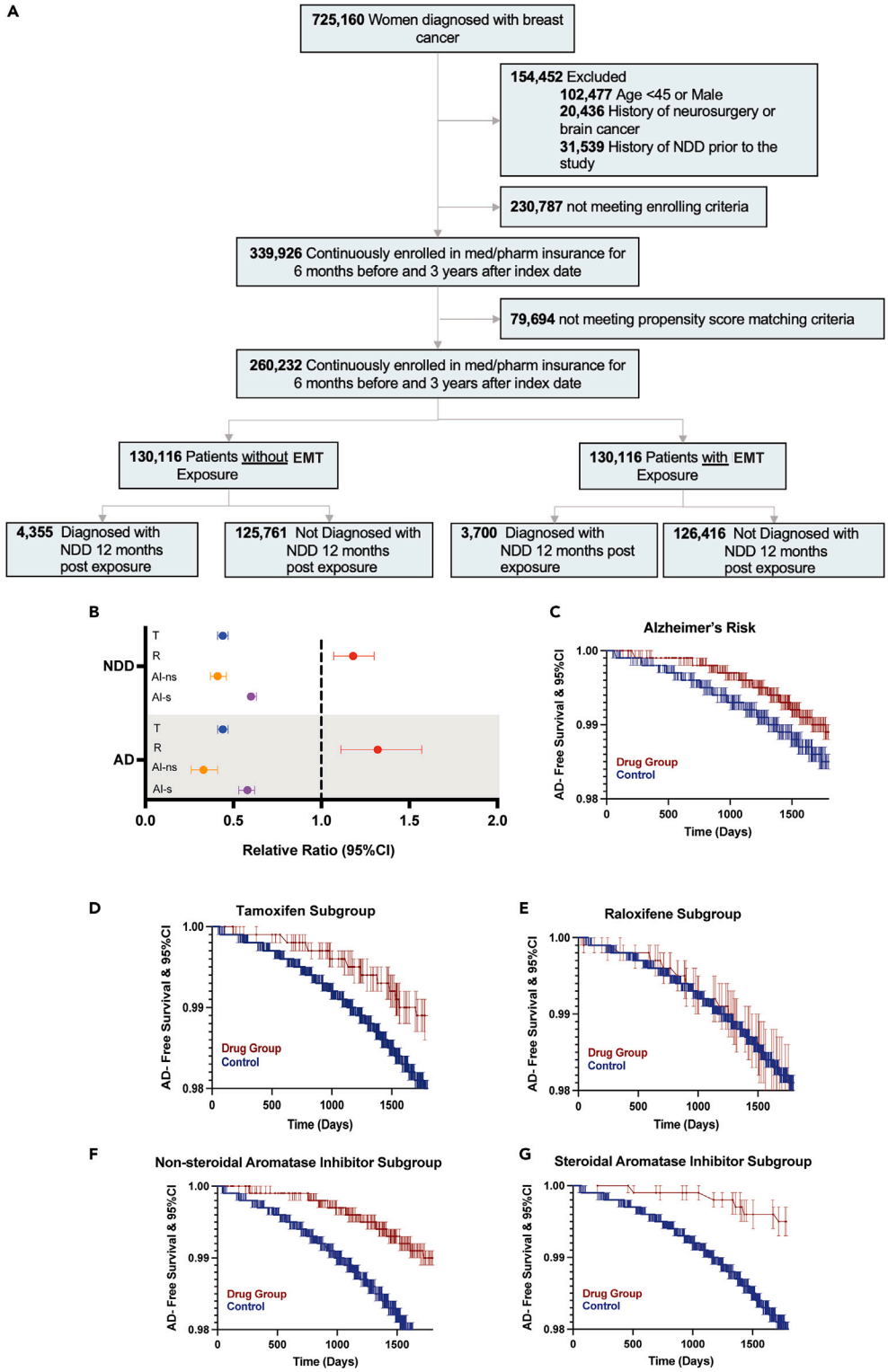

Figure 1. EMT exposure is associated with decreased risk of AD in post-menopausal women being treated for breast cancer

(A) Study design and patient characteristics from the Mariner insurance claims dataset. (B) Odds ratio and 95% CI on AD risk for individual EMT classes (BLUE, tamoxifen; RED, raloxifene; YELLOW, non-steroidal aromatase inhibitors; PURPLE, steroidal aromatase inhibitors).

(C) Kaplan-Meier survival curves for all EMTs for AD-free survival over 5 years.

(D–G) Kaplan-Meier survival Curves for AD-free survival for individual EMT classes.

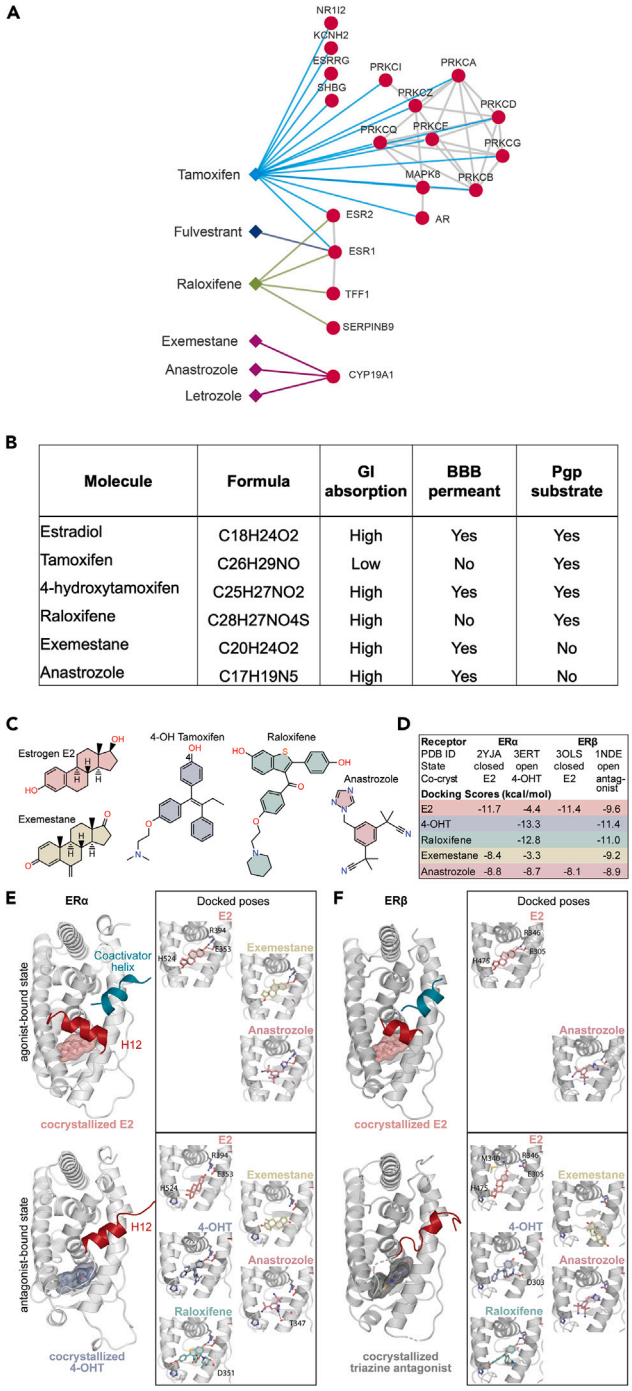

Molecule	Formula	GI absorption	BBB permeant	Pgp substrate
Estradiol	C18H24O2	High	Yes	Yes
Tamoxifen	C26H29NO	Low	No	Yes
4-hydroxytamoxifen	C25H27NO2	High	Yes	Yes
Raloxifene	C28H27NO4S	High	No	Yes
Exemestane	C20H24O2	High	Yes	No
Anastrozole	C17H19N5	High	Yes	No

Receptor	ERα		ERβ	
PDB ID	2YJA	3ERT	3OLS	1NDE
State	closed	open	closed	open
Co-cryst	E2	4-OHT	E2	antag-onist
Docking Scores (kcal/mol)				
E2	-11.7	-4.4	-11.4	-9.6
4-OHT		-13.3		-11.4
Raloxifene		-12.8		-11.0
Exemestane	-8.4	-3.3		-9.2
Anastrozole	-8.8	-8.7	-8.1	-8.9

Figure 2. Estrogen-modulating therapies, protein drug target, and docking predictions of EMT–estrogen receptor interactions in human

(A) Drug-protein network based on DrugBank protein interactors.

(B) Chemical formula of EMTs used for analyses and qualitative pharmacokinetic properties of gastrointestinal absorption, blood-brain barrier (BBB) penetration, and P-glycoprotein (Pgp) multidrug transporter substrate status based on SwissADME.[19] Of note, tamoxifen and raloxifene are not predicted to cross the BBB whereas the active metabolite of tamoxifen (4-OH tamoxifen) is predicted to readily cross the BBB.

(C) Molecular structures of each of the molecules used in analyses of EMTs.

(D) Docking scores for agonist and antagonist-bound states of human ERα and ERβ receptor ligand-binding domains. No docking poses were returned for several ligand-receptor combinations and hence the docking scores are left blank.

(E) Structures of the ligand-binding domain of human ERα shown in ribbon representation. Top: structure with estrogen E2 bound in the hydrophobic cavity and a stapled coactivator helix bound at the coactivator site (PDB ID: 2YJA), Bottom: structure with 4-OHT bound and helix 12 (H12) shifted to the coactivator site (PDB

Figure 2. *Continued*

ID: 3ERT). Insets show the top docked pose for each compound with potential hydrogen bond partners shown as sticks. For clarity, H12 is omitted from inset views. The co-crystallized ligand is shown as black lines for E2 or and 4-OHT, illustrating high congruence of docked poses to experimentally determined ligand conformations.

(F) Representation of the ligand-binding domain of human ERβ ligand-binding domain. Top: structure with estrogen E2 bound in the hydrophobic cavity and a nuclear receptor coactivator 1 helix bound at the coactivator site (PDB ID: 3OLS), Bottom: structure with a triazine antagonist bound and helix 12 (H12) shifted to the coactivator site (PDB ID: 1NDE). Insets show the top docked pose for each compound as in inset E. The co-crystallized ligand is shown as black lines for E2.

To determine whether EMTs crossed the blood-brain barrier, EMT concentration in brain tissue was determined by mass spectrometry. Results of these analyses indicated that EMTs were detectable in both blood and brain at the time of sacrifice. The exception was raloxifene which, while detectable in blood, was below detectable limit in brain indicating poor brain penetration (Figure 3A).

Gene expression analyses were conducted for each treatment group to determine the magnitude and direction of EMT-induced transcriptional activation (Figure 3B). Magnitude of transcriptional response for all conditions was compared to OVX+vehicle. Top activated pathways included oxidative phosphorylation, AMPK, CREB, androgen, and calcium signaling (Figure 3B). Relatively, these pathways were increased compared to sham-OVX control, estradiol, tamoxifen, exemestane, and anastrozole treatment. Of note, the aromatase inhibitors exemestane and anastrozole induced a mixed activation/inhibition profile (Figure 3B). These data are consistent with EMTs, with the exception of raloxifene, activating estrogenic mechanisms across multiple pathways through common and unique transcriptional pathways (Figure 3B).

Results of the transcriptomic analyses indicated several common and unique genes that were upregulated and downregulated in response to EMT treatment (Figure 3C). Individual genes are separated into those most upregulated (log fold change greater than 1) and most downregulated (log fold changes less than −1) with the strongest p values ($p < 0.01$). In Figure 3C, green-colored genes represent common upregulated targets between two classes of EMTs and red-colored genes represent common downregulated targets between two classes of EMTs. Yellow-colored gene targets were upregulated in one class of EMT and downregulated in another class of EMT whereas genes in black were unique to one EMT class. The functions of common genes were primarily associated with regulation of transcription and upstream pathways involving regulation of immune cell recruitment and signaling.

The top 200 genes impacted by EMT treatment, p value less than 0.01, were then used to conduct an enrichment analysis of the related targets to identify significant gene ontology (GO) biological processes characteristics (Figure 3D). While the GO terms included unique biological processes, the overarching themes were predominately neurological and associated with neuronal morphology, neuron electrophysiologic function, as well as bioenergetics.

To validate the impact of EMT on specific neuronal estrogen-dependent genes, rat hippocampal neurons were isolated and treated with EMTs for 24 h and estrogen-responsive transcript levels were analyzed via qPCR arrays using the delta-delta Ct method (Figure 3E). Expression of key estrogen signaling transcript levels after EMT or estrogen treatment was compared to the baseline expression in vehicle-treated neurons relative to housekeeping gene expression (18s, GAPDH, HPRT1, GUSB) (Figure 3E). In rat hippocampal neuron cultures, E2 exposure was associated with increased expression of estrogen response genes including Foxa1, Hsp90, and Vegfa (Figure 3E, first column). The tamoxifen-induced gene expression profile was the most similar to that induced by E2 treatment (Figure 3E, second column). Exemestane and anastrozole treatment induced an expression profile comparable to E2 with a greater magnitude of expression relative to that induced by E2 (Figure 3E, fourth and fifth column). Of note, consistent with the *in vivo* animal data and human informatics data, raloxifene did not induce a profile similar to E2 treatment and was, instead, associated with a decrease in expression of estrogen response genes profile in neurons (Figure 3E, third column).

EMT treatment results in estrogenic profile of neuronal structural morphology

To determine the phenotypic impact of EMT treatment on neuronal morphology, E18 rat hippocampal neurons were isolated and cultured on glass coverslips for 10 days before treatment. On day 10 *in vitro*, hippocampal neurons were treated with EMTs for 24 h followed by fixation and immune labeling for MAP2 and imaged by confocal microscopy. EMT-treated neurons were compared to morphological outcomes under vehicle (0.1% EtOH) and to 17β-estradiol (E2)-treated neurons to determine comparable versus unique phenotypes. EMT dosing was based on published serum levels from women treated for breast cancer for each EMT,[22–25] whereas E2 dosing was based on previously published data relevant to experimental outcomes[8,9,26–34] and functional assay outcomes.[35]

E2-treated neurons exhibited the prototypical phenotype in neuronal morphology which included statistically significant ($p < 0.001$) increases in whole neuron volume, area, number of branches, as well as complexity of the branching pattern compared to the vehicle control-treated cells (Figures 4A, 4B, 4G, 4H, 4I, and 4J). These morphological outcomes are consistent with E2 as a morphological and synaptic plasticity regulator.[36]

EMT treatment, tamoxifen (Figure 4C), raloxifene (Figure 4D), exemestane (Figure 4E), and anastrozole (Figure 4F) resulted in statistically significant increases in morphology (neuron volume, area, number of branches, as well as complexity of the branching pattern; (tamoxifen, raloxifene, exemestane, $p < 0.001$; anastrozole, $p < 0.005$)) compared to vehicle control (Figures 4G, 4H, 4I, and 4J). EMT-induced morphological phenotypes were comparable to and not significantly different from those induced by E2. The comparability between structural plasticity induced by E2 and EMTs is consistent with estrogenic agonist properties.

EMT-treated neurons exhibit an estrogenic electrophysiological profile

To determine functional consequences of EMT morphological profiles, electrophysiological properties were investigated using multi-electrode arrays (MEA) to determine functional connectivity (Figure 4K). Hippocampal neurons were cultured on MEA electrodes for 10 days prior

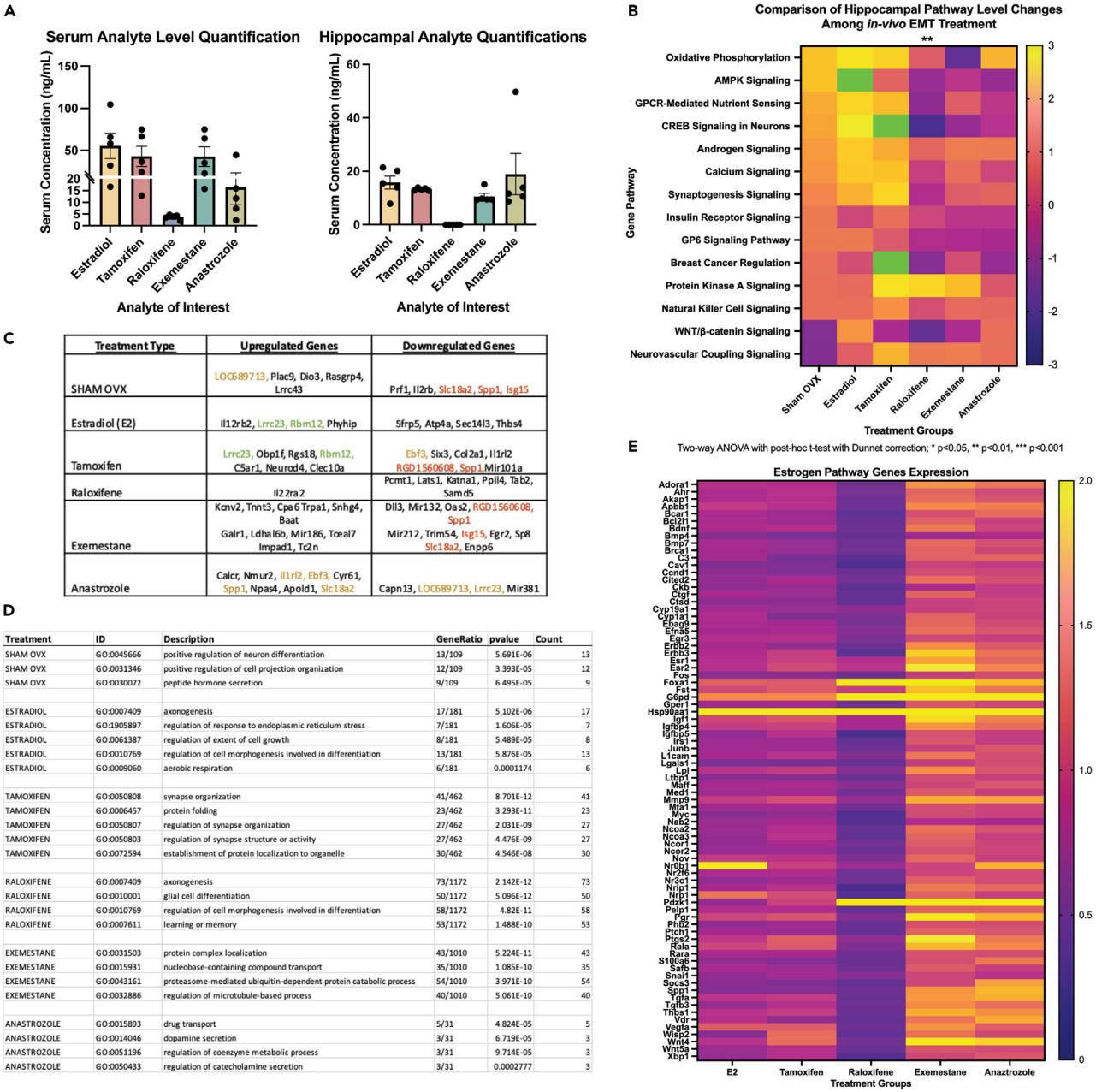

Treatment	ID	Description	GeneRatio	pvalue	Count
SHAM OVX	GO:0045666	positive regulation of neuron differentiation	13/109	5.691E-06	13
SHAM OVX	GO:0031346	positive regulation of cell projection organization	12/109	3.393E-05	12
SHAM OVX	GO:0030072	peptide hormone secretion	9/109	6.495E-05	9
ESTRADIOL	GO:0007409	axonogenesis	17/181	5.102E-06	17
ESTRADIOL	GO:1905897	regulation of response to endoplasmic reticulum stress	7/181	1.606E-05	7
ESTRADIOL	GO:0061387	regulation of extent of cell growth	8/181	5.489E-05	8
ESTRADIOL	GO:0010769	regulation of cell morphogenesis involved in differentiation	13/181	5.876E-05	13
ESTRADIOL	GO:0009060	aerobic respiration	6/181	0.0001174	6
TAMOXIFEN	GO:0050808	synapse organization	41/462	8.701E-12	41
TAMOXIFEN	GO:0006457	protein folding	23/462	3.293E-11	23
TAMOXIFEN	GO:0050807	regulation of synapse organization	27/462	2.031E-09	27
TAMOXIFEN	GO:0050803	regulation of synapse structure or activity	27/462	4.476E-09	27
TAMOXIFEN	GO:0072594	establishment of protein localization to organelle	30/462	4.546E-08	30
RALOXIFENE	GO:0007409	axonogenesis	73/1172	2.142E-12	73
RALOXIFENE	GO:0010001	glial cell differentiation	50/1172	5.096E-12	50
RALOXIFENE	GO:0010769	regulation of cell morphogenesis involved in differentiation	58/1172	4.82E-11	58
RALOXIFENE	GO:0007611	learning or memory	53/1172	1.488E-10	53
EXEMESTANE	GO:0031503	protein complex localization	43/1010	5.224E-11	43
EXEMESTANE	GO:0015931	nucleobase-containing compound transport	35/1010	1.085E-10	35
EXEMESTANE	GO:0043161	proteasome-mediated ubiquitin-dependent protein catabolic process	54/1010	3.971E-10	54
EXEMESTANE	GO:0032886	regulation of microtubule-based process	40/1010	5.061E-10	40
ANASTROZOLE	GO:0015893	drug transport	5/31	4.824E-05	5
ANASTROZOLE	GO:0014046	dopamine secretion	3/31	6.719E-05	3
ANASTROZOLE	GO:0051196	regulation of coenzyme metabolic process	3/31	9.714E-05	3
ANASTROZOLE	GO:0050433	regulation of catecholamine secretion	3/31	0.0002777	3

Figure 3. Comparison of hippocampal pathway changes in response to *in vivo* EMT treatment

(A) Serum and brain levels of estradiol and EMT following *in vivo* treatment in OVX rats. (B) Heatmap representing fold-change expression within signaling pathways relative to vehicle treatment. Green represents fold change greater than 3-fold. (C) Top upregulated and downregulated genes for each treatment type relative to vehicle. (D) Gene Ontology pathway changes for each treatment group where count is the number of genes for each given pathway. (E) Gene expression of E2-dependent genes post EMT treatment in hippocampal E18 neurons by qRT-PCR. For each heatmap, each vertical column represents one of the EMT treatments in the OVX rats or the SHAM OVX vehicle treatment group.

to E2 or EMT treatment as in the morphologic experiments followed by roster spike recording (Figures 4K and 4L). E2 induced an increase in neuronal burst firing that was consistent with published electrophysiological properties[37–39] with E2 exposure increasing both the number of spikes per burst and duration of the burst ($p < 0.001$) compared to control. E2 exposure did not impact the overall spike count of the neurons, rather, E2 decreased ($p < 0.001$) the inter-spike interval (ISI), which is consistent with an increase in the number of postsynaptic connections[40] (Figure 4M). Importantly, E2 did not increase the inter-burst interval, a proxy for overall frequency of burst type firing (Figure 4N). The increase in electrophysiological excitability and synaptic activity are consistent with predicted functional outcomes of E2-induced neuronal morphological complexity (Figures 4A–4F).

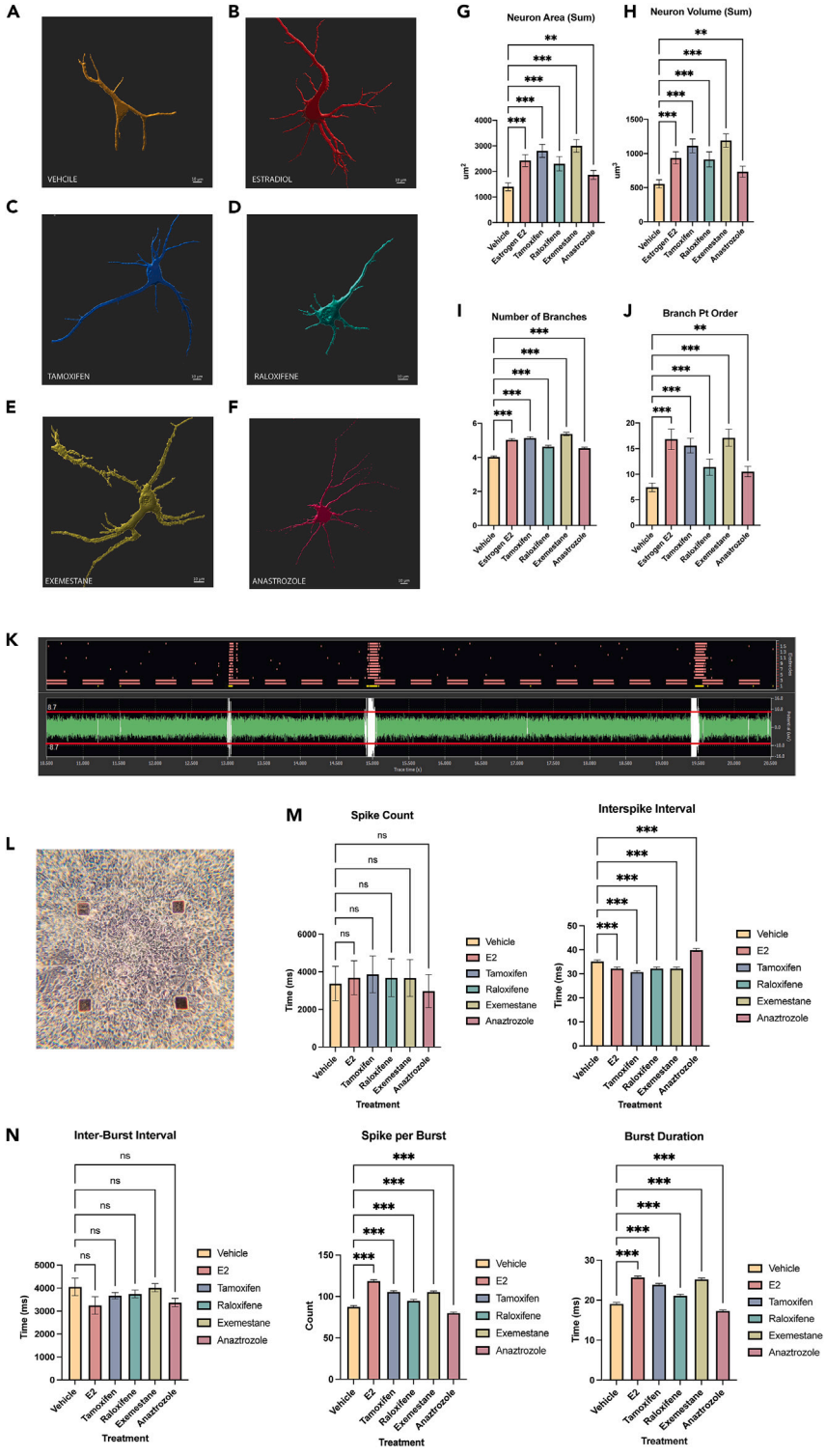

Figure 4. Estrogen-modulating therapies induced estrogenic neuronal morphology and electrophysiological phenotypes

(A–F) Representative rat hippocampal neurons for morphological analysis following 24 h of treatment for (A) vehicle, (B) estradiol (10 ng/mL), (C)tamoxifen (10 ng/mL), (D) raloxifene (1 pg/mL), (E) exemestane (5 ng/mL), and (F) anastrozole (10 ng/mL).

(G–I) Quantification of morphological analyses which are the average of outcomes from three independent experiments with three replicates per treatment, n = 50 neurons per experimental treatment.

Figure 4. *Continued*

(K) Representative roster spike plot to assess electrophysiological phenotype. (L) Representative image of neuronal density on multi-electrode arrays. (M) Quantification of single spike recordings for each EMT treatment. (N) Quantification of burst spike recordings for each EMT treatment. Data are the average of three independent experiments with three replicates per treatment over 5 min of recording. (*$p < 0.05$, **$p < 0.005$, ***$p < 0.001$).

Comparison of EMT impact on electrophysiological phenotype indicated that each EMT exerted electrophysiologic characteristics comparable to E2 with the exception of anastrozole (Figures 4M and 4N). Comparable to E2, tamoxifen, raloxifene, and exemestane treatment did not impact neuronal spike number and like E2 decreased the ISI ($p < 0.001$) which is suggestive of an increase in the number of postsynaptic connections (Figure 4M). Treatment with the aforementioned EMTs was also associated with an increase in neuronal burst firing similar to E2 in which treatment increased both the number of spikes per burst and burst duration ($p < 0.001$) compared to control (Figure 4N). These electrophysiological parameters were not statistically different than E2 treatment suggesting an estrogen agonist effect of tamoxifen on neuronal firing profiles. Anastrozole, unlike the other EMTs, impacted the aforementioned electrophysiologic phenotypes but in the opposite direction and magnitude of the changes generated by other EMT treatment (Figures 4M and 4N).

EMT-treated neurons exhibit estrogenic mitochondrial bioenergetic profile

Estrogen-induced increase in neural circuitry and synaptic activation is accompanied by a commensurate increase in mitochondrial oxidative phosphorylation and ATP generation.[36,41–47] To determine whether EMTs exerted mitochondrial respiratory properties comparable to E2, hippocampal neurons treated with EMTs followed by assessment of mitochondrial respiratory properties and capacity.

Compared to vehicle, E2 increased mitochondrial maximal respiration ($p < 0.05$), ATP production ($p < 0.05$), and coupling efficiency ($p < 0.05$) in hippocampal neurons (Figure 5A, 5D, 5E, and 5H). E2 treatment did not change basal respiration, spare respiratory capacity, or proton leak in neurons (Figures 5A, 5C, 5F, and 5G). These changes are consistent with known estrogen action on the mitochondrial function in neurons.[46] EMTs induced similar respiratory profiles to that of E2-treated neurons with notable exceptions. For the extracellular acidification rate (ECAR), a proxy for anaerobic glycolysis, E2 and all EMTs, with the exception of anastrozole, induced an increase in ECAR consistent with a decrease in anaerobic glycolysis (Figure 5B). All EMTs increased maximal respiration and ATP production ($p < 0.005$, $p < 0.001$ for exemestane) (Figures 5D and 5E). Unlike E2, raloxifene did not induce an increase in spare respiratory capacity (Figures 5A and 5F). Exemestane was the only EMT to increase basal respiration (Figures 5A and 5C).

EMT-treated neurons induce estrogenic agonism impacting mitochondrial bioenergetics and biogenesis

To determine the impact of EMT on mitochondrial biogenesis and morphology, E18 rat hippocampal neurons were isolated and cultured for 10 days prior to treatment followed by 24-h treatment with either E2 or EMTs. Mitochondrial respiration and morphology in EMT-treated neurons were compared to vehicle and to E2-treated neurons.

Estrogen induced a statistically significant increase ($p < 0.01$) in the number of TOM20-positive mitochondria per 100 μm^3 (Figures 5I and 5J), which was paralleled by a shift toward smaller volume mitochondria consistent with increased fission and increased mitochondria number (Figures 5I and 5J). Much like E2, tamoxifen, exemestane, and anastrozole-treated neurons (Figure 5K) exhibited an estrogenic response with an increased number of TOM20-positive mitochondria per 100 μm^3 ($p < 0.01$) (Figures 5I and 5J) and a shift in the size of the mitochondria toward smaller volumes indicative of increased mitochondrial fission (Figures 5I and 5J). Unlike E2, raloxifene (Figure 5K), and the other EMTs, did not significantly impact mitochondrial number although raloxifene did promote a smaller size of mitochondria similar to the other EMTs (Figures 5I and 5J).

DISCUSSION

Age is the greatest risk factor for breast cancer, as 80% of diagnoses occur at ages 45 or older.[2,3,48] In parallel, age is the greatest risk factor for Alzheimer's disease with two-thirds of persons with the disease being women.[49] As females have a higher lifetime risk for late-onset AD[49] and given the association between estrogen loss and increased AD risk,[42,47] questions regarding the impact and brain-specific mechanism of therapies known to antagonize estrogen action systemically are of clinical relevance. To address the impact of pharmacological breast cancer therapies on risk of AD, we conducted a medical informatic analysis of women receiving breast cancer therapy and the associated risk of developing AD. Importantly, these results add to the growing literature of EMTs and association of decreased risk of AD. The published reports regarding EMTs and AD disease risk are mixed[17,18,50–53] and thus warranted further investigation of fundamental mechanisms by which these agents could exert their effects in brain. We followed these clinically based analyses with a series of translational analyses to address potential mechanisms underlying the medical informatic data indicating that EMTs were associated with a seemingly counterintuitive decreased risk of AD in post-menopausal women with breast cancer. We reasoned that one potential mechanism by which EMT may exert a reduced risk of AD is through activation of estrogenic pathways in brain comparable to those induced by estrogen.

Herein, we report the largest-to-date retrospective analysis regarding the impact of EMT on AD risk in women 45 years or older with breast cancer. Results of the medical informatic analysis indicated that, similar to estrogen replacement,[54,55] EMT exposure was associated with a reduced risk of AD. The data reported herein, which were derived from an independent clinical population, replicated previous reports.[17,18] Specifically, results of the medical informatics analyses are consistent in replicating that exposure to EMTs, specifically tamoxifen and the aromatase inhibitors, is associated with a reduced risk of AD. Raloxifene exposure in this cohort was associated with increased risk of AD, which may be due, in part, to dosing and pharmacokinetic qualities of raloxifene, where previous studies reported that raloxifene is associated with a

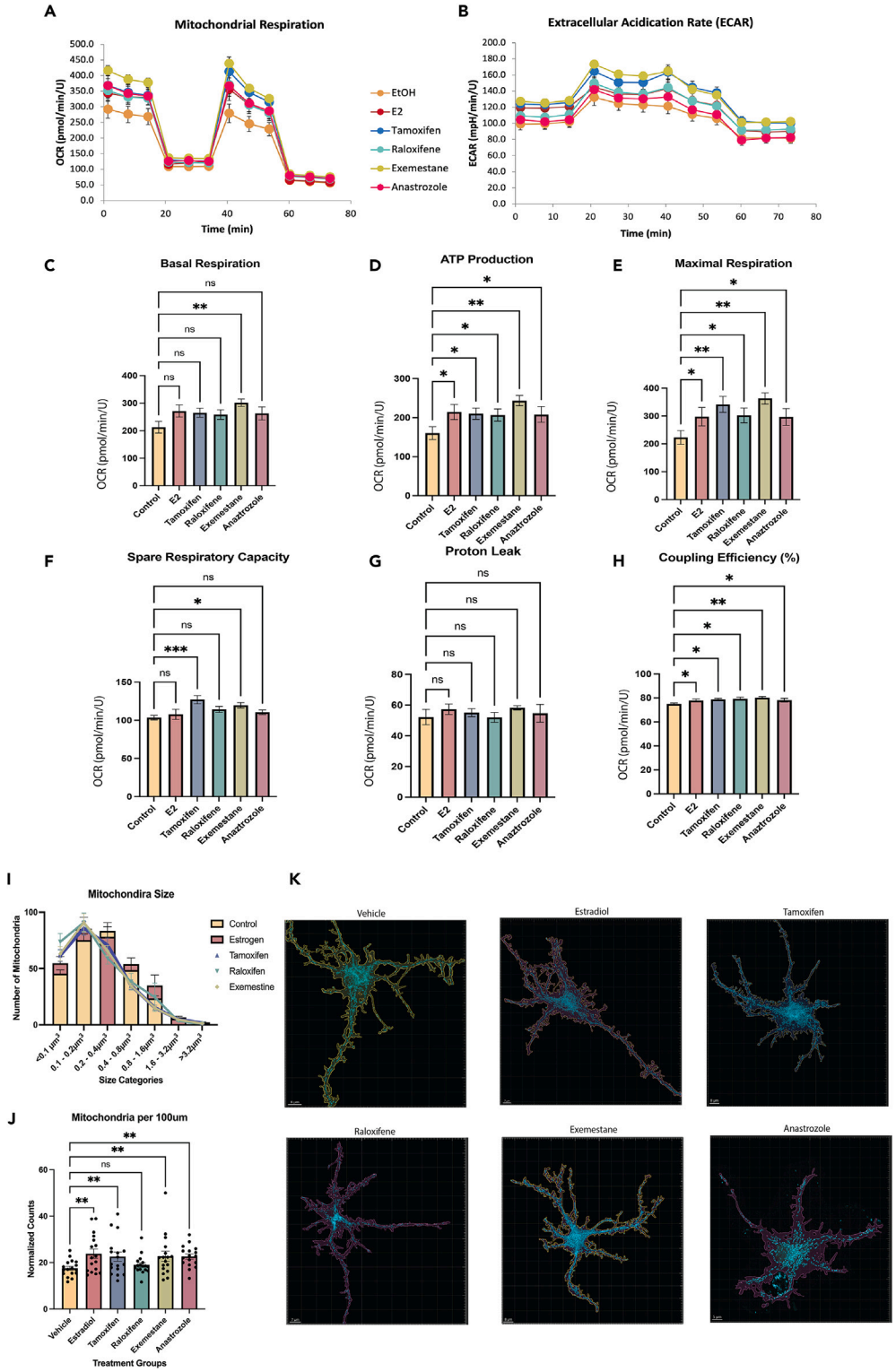

Figure 5. Estrogen-modulating therapies elicit estrogen agonism in mitochondrial function in rat hippocampal neurons

(A) Mitochondrial respiration plots from EMT treatments. (B) Extracellular acidification rate graph. (C–H) Bar graphs representing components of mitochondrial respiration-derived OCR plots. (I) Mitochondrial size secondary to EMT treatments. (J) Mitochondrial counts per 100 μm^3.

(K) Representative images of EMT-treated neurons labeled for TOM20 for mitochondrial analysis and b-actin for structural comparison. (*$p < 0.05$, **$p < 0.005$, ***$p < 0.001$).

reduced risk of AD only at higher doses than that used clinically for breast cancer.[56,57] A recent clinical report investigating the association between tamoxifen and raloxifene exposure and mild cognitive impairment (MCI) among women with and without a history of breast cancer demonstrated that women treated with these agents did not have an increased risk of MCI, or demonstrate any structural MRI markers of neurodegeneration.[58] These results are consistent with our findings of decreased risk of AD and preventative efficacy of tamoxifen[18] and are an independent validation of this observation in a distinct population cohort.

The computational chemistry analysis replicates previous reports of EMT targets[4,59] and expands the mechanism of action of these therapeutics.[4,59] We show that there exist both novel and overlapping targets for each of the EMTs and that, apart from raloxifene, each EMT or active metabolite, in the case of tamoxifen, is predicted to readily cross the BBB and therefore elicit pharmacodynamic action in brain. The computational modeling of EMTs with ERα and ERβ predicts interaction of aromatase inhibitors with estrogen receptors. Of note, it is also possible that EMTs may be acting, either independently or in addition to their direct receptor function through non-genomic action involving coregulatory epigenetic changes involving heterodimeric interactions between the receptor subtypes consistent with receptor-level changes seen in estrogen receptor in breast cancer.[60–63]

Whether acting via direct nuclear effects, indirect non-nuclear actions, or a combination of both, the effects of estrogens on gene expression are controlled by highly regulated complex mechanisms.[64] For example, estrogen-dependent transient receptor potential cation channel, subfamily V, member 1 expression induces neuroprotection, neurogenesis, and regeneration on damaged tissues.[65] It is likely that the effects of estrogens on cognitive performance are due to rapid mechanisms, including mechanisms that influence Ca^{2+} homeostasis dynamics, provide protection against neurotoxic insults, and reduce inflammatory signals from neural tissues.[66,67] Of note, the pathways by which EMT are working to modulate in the hippocampus are well-documented pathways connecting the loss of estrogen action to AD pathobiology. The EMT-induced transcriptomic profiles are consistent with estrogenic pathways that sustain brain health, neurological function, and reduced risk of AD.[41,68,69] Multiple cellular and molecular mechanisms underlying estrogen-inducible promotion of cognitive function and neuronal survival have been proposed in a wide range of cell types.[68,70] 17β-estradiol (E2) is known to work through a plasma membrane-associated endoplasmic reticulum (ER) that activates the phosphatidylinositol 3-kinase[71] which in turn activates Ca^{2+}-independent protein kinase C (PKC).[72] Next, a Ca^{2+}-independent PKC isoform phosphorylates the L-type Ca^{2+} channel followed by Ca^{2+} influx[73] which activates conventional Ca^{2+}-dependent PKCs,[74] which then phosphorylate and activate Src kinase.[75] Src then activates the MEK/ERK1/2 pathway[76] followed by translocation of activated ERK into the nucleus.[77] Subsequent to CREB activation by activated ERK phosphorylation, the Src/ERK signaling cascade leads to potentiation of glutamate-dependent activation of AMPA and NMDA receptors.[78]

Individual gene expression profiles across the various EMTs could elucidate differences in the neuro-clinical benefits seen from exposure during breast cancer treatment. For example, common targets increased by EMT treatment included Foxa1, VEGFA, Tgfa, Mmp9, and Igf1 expression levels. These genes are of interest due to their known biological actions. Foxa1 is associated with control of glucose homeostasis via PEPCK signaling and epigenetic regulation of key glycolytic enzymes. VEGFA induces endothelial cell proliferation, promotes cell migration, inhibits apoptosis, and induces permeabilization of blood vessels. Tgfa, Mmp9, and Igf1 are all genes related to inflammatory processing and the regulation of neuroinflammation signaling throughout the aging process.[79] These genes are common targets of both estradiol and EMT treatment and are mechanistically linked to prodromal risk cascades of AD that are modulated by estrogen which could represent both classical and non-classical ER downstream network activation. Unpublished docking data from our group suggest potential interaction between these testosterone and androstenedione and multiple estrogen receptor subtypes. Conversely, there is the possibility that the observed effect of aromatase inhibitors may be due, in part, to an effect of testosterone and androstenedione on the androgen receptor.

It is well documented that ERα and ERβ1 share an affinity for multiple estrogenic molecules, estrogen antagonists, and EMTs[80] to regulate genes through the nuclear estrogen response element.[81] Remarkably, ERα and ERβ1 differ in their ability to regulate transcription via the AP-1 response element.[82] For example, 17β-estradiol, as well as several antiestrogens, activates transcription through interactions of ERα with AP-1; however, in the context of ERβ1 acting through AP-1, 17β-estradiol fails to activate transcription whereas anti-estrogens activated transcription.[81] The molecular docking data indicate that both SERMs and aromatase inhibitors can interact with estrogen receptors in brain with drug-specific receptor affinities.

A series of reverse translational comparative analyses between the effects of EMT and 17β-estradiol in both *in vivo* rat brain and rat hippocampal neuron cultures demonstrated that EMTs exert pro-estrogen effects. Results from the cell data suggest activation of ER pathways in brain and receptor-specific affinities for individual EMTs consistent with previous reports.[64,83] Building on these findings, the results of the *in vivo* rat studies demonstrated pathway-level changes consistent with activation of estrogen receptor pathways relevant to AD prevention and brain function. Historically, tamoxifen has garnered attention not only for its established role in breast cancer treatment but also for its use in transgenic mouse models. Consistent with data presented herein, previous reports have indicated that tamoxifen influences gene expression within the brain, potentially leading to neuroprotective effects and cognitive modulation.[84–88] For instance, tamoxifen administration in animal models led to significant alterations in hippocampal gene expression patterns, particularly those related to synaptic plasticity,[89–93] neuronal survival,[89–93] neuroinflammation,[94] and neuroprotection.[89–94] Collectively, these findings support the neural impact of tamoxifen as a partial estrogen agonist in brain that are consistent with reduction of AD risk in women.

Data reported herein also provide a pharmacokinetic rationale for the conflicting reports of the association of raloxifene with AD, likely due to poor brain penetration at clinical doses and treatment duration[56,57,95] while validating early reports that tamoxifen and its metabolites are brain penetrant.[96,97] Finally, direct experimentation with EMT and rat neurons demonstrated engagement with key estrogen-activated pathways associated with neuronal health and function.[36] EMT treatment was associated with an estrogen-like promotion and maintenance of neuron morphology, electrophysiology, and mitochondrial function all known to be impacted in AD pathogenesis.[36,47] These results validate

at a molecular level the MRI findings from previous reports indicating that these therapies do not increase AD risk or accelerate the degenerative process.[58] Recent reports in non-excitable tissue, such as breast, suggest that there may be morphological and electrophysiological properties of EMTs that share features of neural tissue response.[98–100] These findings add to the literature documenting EMT pharmacological action in organs such as breast and uterine tissue and the well-known tissue-specific and divergent mechanism of EMTs.[6,100,101]

Limitations of the study

A challenge of translational mechanistic research is how best to model the complexity of the human condition. Herein, we employed multiple investigational approaches to incorporate levels of complexity into a reverse translational study of prevention observations including the use of human clinical data, human cell lines, rodent cell lines, and *in vivo* rodent studies. However, there remain limitations to this approach. The medical informatic data reported are generated from a retrospective analysis of a medical claims database and thus there could be factors, known and unknown, that even with propensity matching may not be adequately addressed which we attempted to address through our study design. The patients included may have obtained services outside of those included in this database. In addition, EMT exposure was assessed by filled prescription charges, indicating that the EMT was obtained by a patient. However, data on specific breast pathologic condition or contraindications for therapy cannot be assessed in this dataset. The factors associated with nonadherence include perception of a low risk of recurrence, adverse effects (perceived or real), costs, suboptimal patient-physician communication, and lack of social support. Additionally, we did not include in this study data regarding non-hormonal therapies such as chemotherapy or radiotherapy; however, in our earlier report, non-hormonal therapies were not effective for reducing risk of AD.[17,18] Additionally, medication adherence in this study was calculated using prescription refill records which in some cases may overestimate the adherence rate. The cell-based assays relied predominately on rat hippocampal neurons which limit the analysis of the contribution of other cell types in the hippocampus. Thus, follow-up in non-neuron cell types and other brain regions is warranted.

Conclusions

Aging of the global population will contribute to risk of both breast cancer and Alzheimer's disease in women.[2,3,48,49,102] As EMTs are the first-line pharmacological strategy to reduce breast cancer recurrence,[5,103] we conducted medical informatic analyses to determine the impact of EMTs on risk of Alzheimer's disease in women with breast cancer. Outcomes of these analyses indicated a reduced risk of neurodegenerative diseases in the aggregate and specifically Alzheimer's in women receiving either tamoxifen or aromatase inhibitors. The reduced risk of Alzheimer's disease in tamoxifen and aromatase inhibitor users suggested that these molecules, which were developed to reduce estrogen action in the breast, could exert an estrogenic effect in brain. Outcomes of a broad set of computational, molecular, and physiological analyses indicate that tamoxifen and aromatase inhibitors exerted estrogenic action in neural cells and brain which could account for the reduced risk of a neurodegenerative disease. Collectively, these findings provide both population level and mechanistic data to inform clinical decision-making regarding use of EMTs for secondary prevention of breast cancer recurrence while also considering the long-term impact on brain health and risk of age-associated neurodegenerative diseases including Alzheimer's. Further investigation of the molecular mechanism of EMTs in brain with respect to functional interactions with the nuclear estrogen receptors ER-α and ER-β, the membrane GPER1 receptor, as well as non-classical receptors will be increasingly important to our understanding of the impact of estrogen modulation on degenerative diseases of the nervous system and could improve patient compliance given the growing concern of neurological impairment in aging populations.

STAR★METHODS

Detailed methods are provided in the online version of this paper and include the following:

- KEY RESOURCES TABLE
- RESOURCE AVAILABILITY
  - Lead contact
  - Materials availability
  - Data and code availability
- EXPERIMENTAL MODEL AND STUDY PARTICIPANT DETAILS
- METHOD DETAILS
  - Medical informatics: Data source
  - Medical informatics: Study design and variables
  - Medical informatics: Statistical analysis
  - Animal use
  - Cell culture
  - Computation molecular modeling and docking of SERMs and estrogen receptors
  - *In-vivo* EMT treatment
  - RNA isolation
  - Real-time quantitative PCR assays
  - Bulk RNA sequencing (RNA-Seq)

- Ingenuity pathway analysis (IPA) of RNA-Seq and biological pathway analysis
- QUANTIFICATION AND STATISTICAL ANALYSIS
  - Medical informatics
  - General statistical analysis

SUPPLEMENTAL INFORMATION

Supplemental information can be found online at https://doi.org/10.1016/j.isci.2023.108316.

ACKNOWLEDGMENTS

We would like to thank Wade Chew and Sherry Chow, Ph.D., for their insights and method development for the mass spectrometry analysis of E2 and EMT levels in serum and brain and acknowledge both the Vanderbilt VANTAGE Core and University of Arizona Cancer Center MassSpec Core. The graphical abstract figure was created with BioRender.com.

R.D.B. was funded by National Institute on Aging grants P01AG026572, T32AG061897, and R37AG053589 and Women's Alzheimer's Movement grant.

The National Institutes of Health and the Women's Alzheimer's Movement Foundation had no role in the design and conduct of the study; collection, management, analysis, and interpretation of the data; preparation, review, or approval of the manuscript; and decision to submit the manuscript for publication.

AUTHOR CONTRIBUTIONS

Conceptualization, G.L.B. and R.D.B.; methodology, G.L.B., G.T.-H., S.C., Y.S., S.P.-M., Z.M., M.P.-R., and H.C.-F.; investigation, G.L.B., G.T.-H., S.C., M.P.-R., and F.V.; visualization, G.L.B., G.T.-H.,F.V., S.P.-M., and R.D.B.; funding acquisition, R.D.B.; project administration, R.D.B.; supervision, G.L.B. and R.D.B.; writing – original draft, G.L.B. and R.D.B.; writing – review & editing, G.L.B. and R.D.B.

DECLARATION OF INTERESTS

The authors declare that they have no competing interests.

INCLUSION AND DIVERSITY

We support inclusive, diverse, and equitable conduct of research.

Received: July 27, 2023
Revised: September 8, 2023
Accepted: October 20, 2023
Published: October 24, 2023

REFERENCES

1. N.A. Howlader N, M. Krapcho, D. Miller, A. Brest, M. Yu, J. Ruhl, Z. Tatalovich, A. Mariotto, D.R. Lewis, and H.S. Chen, et al., eds. (2019). SEER Cancer Statistics Review, 1975-2016 (National Cancer Institute), based on November 2018 SEER data submission, posted to the SEER web site. https://seer.cancer.gov/csr/1975_2016/.
2. Siegel, R.L., Miller, K.D., and Jemal, A. (2019). Cancer statistics, 2019. CA. Cancer J. Clin. *69*, 7–34. https://doi.org/10.3322/caac.21551.
3. Rojas, K., and Stuckey, A. (2016). Breast Cancer Epidemiology and Risk Factors. Clin. Obstet. Gynecol. *59*, 651–672. https://doi.org/10.1097/grf.0000000000000239.
4. Miller, W.R. (2003). Aromatase inhibitors: mechanism of action and role in the treatment of breast cancer. Semin. Oncol. *30*, 3–11. https://doi.org/10.1016/s0093-7754(03)00302-6.
5. Visvanathan, K., Hurley, P., Bantug, E., Brown, P., Col, N.F., Cuzick, J., Davidson, N.E., Decensi, A., Fabian, C., Ford, L., et al. (2013). Use of pharmacologic interventions for breast cancer risk reduction: American Society of Clinical Oncology clinical practice guideline. J. Clin. Oncol. *31*, 2942–2962. https://doi.org/10.1200/JCO.2013.49.3122.
6. Hu, R., Hilakivi-Clarke, L., and Clarke, R. (2015). Molecular mechanisms of tamoxifen-associated endometrial cancer (Review). Oncol. Lett. *9*, 1495–1501. https://doi.org/10.3892/ol.2015.2962.
7. Polin, S.A., and Ascher, S.M. (2008). The effect of tamoxifen on the genital tract. Cancer Imag. *8*, 135–145. https://doi.org/10.1102/1470-7330.2008.0020.
8. O'Neill, K., Chen, S., and Brinton, R.D. (2004). Impact of the selective estrogen receptor modulator, raloxifene, on neuronal survival and outgrowth following toxic insults associated with aging and Alzheimer's disease. Exp. Neurol. *185*, 63–80. https://doi.org/10.1016/j.expneurol.2003.09.005.
9. O'Neill, K., Chen, S., and Diaz Brinton, R. (2004). Impact of the selective estrogen receptor modulator, tamoxifen, on neuronal outgrowth and survival following toxic insults associated with aging and Alzheimer's disease. Exp. Neurol. *188*, 268–278. https://doi.org/10.1016/j.expneurol.2004.01.014.
10. Rey, J.R.C., Cervino, E.V., Rentero, M.L., Crespo, E.C., Alvaro, A.O., and Casillas, M. (2009). Raloxifene: mechanism of action, effects on bone tissue, and applicability in clinical traumatology practice. Open Orthop. J. *3*, 14–21. https://doi.org/10.2174/1874325000903010014.
11. National Comprehensive Cancer Network (NCCN) (2019). Practice Guidelines in Oncology: Breast Cancer. Version 2.2017. www.nccn.org.
12. Chen, W.Y. (2019). Selective estrogen receptor modulators and aromatase inhibitors for breast cancer prevention. UpToDate. https://www.uptodate.com/contents/selective-estrogen-receptor-modulators-and-aromatase-inhibitors-for-breast-cancer-prevention.
13. Diaz Brinton, R., Chen, S., Montoya, M., Hsieh, D., Minaya, J., Kim, J., and Chu, H.-P. (2000). The women's health initiative estrogen replacement therapy is neurotrophic and neuroprotective. Neurobiol. Aging *21*, 475–496.
14. Cholerton, B., Gleason, C.E., Baker, L.D., and Asthana, S. (2002). Estrogen and Alzheimer's disease: the story so far. Drugs

Aging *19*, 405–427. https://doi.org/10.2165/00002512-200219060-00002.

15. Deroo, B.J., and Korach, K.S. (2006). Estrogen receptors and human disease. J. Clin. Invest. *116*, 561–570. https://doi.org/10.1172/JCI27987.
16. Han, X., Aenlle, K.K., Bean, L.A., Rani, A., Semple-Rowland, S.L., Kumar, A., and Foster, T.C. (2013). Role of estrogen receptor alpha and beta in preserving hippocampal function during aging. J. Neurosci. *33*, 2671–2683. https://doi.org/10.1523/JNEUROSCI.4937-12.2013.
17. Blanchette, P.S., Lam, M., Le, B., Richard, L., Shariff, S.Z., Pritchard, K.I., Raphael, J., Vandenberg, T., Fernandes, R., Desautels, D., et al. (2020). The association between endocrine therapy use and dementia among post-menopausal women treated for early-stage breast cancer in Ontario, Canada. J. Geriatr. Oncol. *11*, 1132–1137. https://doi.org/10.1016/j.jgo.2020.05.009.
18. Branigan, G.L., Soto, M., Neumayer, L., Rodgers, K., and Brinton, R.D. (2020). Association Between Hormone-Modulating Breast Cancer Therapies and Incidence of Neurodegenerative Outcomes for Women With Breast Cancer. JAMA Netw. Open *3*, e201541. https://doi.org/10.1001/jamanetworkopen.2020.1541.
19. Daina, A., Michielin, O., and Zoete, V. (2017). SwissADME: a free web tool to evaluate pharmacokinetics, drug-likeness and medicinal chemistry friendliness of small molecules. Sci. Rep. *7*, 42717. https://doi.org/10.1038/srep42717.
20. Shiau, A.K., Barstad, D., Loria, P.M., Cheng, L., Kushner, P.J., Agard, D.A., and Greene, G.L. (1998). The structural basis of estrogen receptor/coactivator recognition and the antagonism of this interaction by tamoxifen. Cell *95*, 927–937. https://doi.org/10.1016/s0092-8674(00)81717-1.
21. Brzozowski, A.M., Pike, A.C., Dauter, Z., Hubbard, R.E., Bonn, T., Engström, O., Ohman, L., Greene, G.L., Gustafsson, J.A., and Carlquist, M. (1997). Molecular basis of agonism and antagonism in the oestrogen receptor. Nature *389*, 753–758. https://doi.org/10.1038/39645.
22. Furlanut, M., Franceschi, L., Pasqual, E., Bacchetti, S., Poz, D., Giorda, G., and Cagol, P. (2007). Tamoxifen and its main metabolites serum and tissue concentrations in breast cancer women. Ther. Drug Monit. *29*, 349–352. https://doi.org/10.1097/FTD.0b013e318067ded7.
23. Hochner-Celnikier, D. (1999). Pharmacokinetics of raloxifene and its clinical application. Eur. J. Obstet. Gynecol. Reprod. Biol. *85*, 23–29. https://doi.org/10.1016/s0301-2115(98)00278-4.
24. Hertz, D.L., Kidwell, K.M., Seewald, N.J., Gersch, C.L., Desta, Z., Flockhart, D.A., Storniolo, A.M., Stearns, V., Skaar, T.C., Hayes, D.F., et al. (2017). Polymorphisms in drug-metabolizing enzymes and steady-state exemestane concentration in postmenopausal patients with breast cancer. Pharmacogenomics J. *17*, 521–527. https://doi.org/10.1038/tpj.2016.60.
25. Regenthal, R., Voskanian, M., Baumann, F., Teichert, J., Brätter, C., Aigner, A., and Abraham, G. (2018). Pharmacokinetic evaluation of a transdermal anastrozole-in-adhesive formulation. Drug Des. Devel. Ther. *12*, 3653–3664. https://doi.org/10.2147/DDDT.S170764.
26. Halbreich, U., and Kahn, L.S. (2000). Selective oestrogen receptor modulators–current and future brain and behaviour applications. Expert Opin. Pharmacother. *1*, 1385–1398. https://doi.org/10.1517/14656566.1.7.1385.
27. Tang, M.-X., Jacobs, D., Stern, Y., Marder, K., Schofield, P., Gurland, B., Andrews, H., and Mayeux, R. (1996). Effect of oestrogen during menopause on risk and age at onset of Alzheimer's disease. Lancet *348*, 429–432.
28. Zhao, L., Mao, Z., Chen, S., Schneider, L.S., and Brinton, R.D. (2013). Early intervention with an estrogen receptor β-selective phytoestrogenic formulation prolongs survival, improves spatial recognition memory, and slows progression of amyloid pathology in a female mouse model of Alzheimer's disease. J. Alzheimers Dis. *37*, 403–419. https://doi.org/10.3233/jad-122341.
29. Brinton, R.D., Proffitt, P., Tran, J., and Luu, R. (1997). Equilin, a principal component of the estrogen replacement therapy premarin, increases the growth of cortical neurons via an NMDA receptor-dependent mechanism. Exp. Neurol. *147*, 211–220. https://doi.org/10.1006/exnr.1997.6619.
30. Chen, S., Nilsen, J., and Brinton, R.D. (2006). Dose and temporal pattern of estrogen exposure determines neuroprotective outcome in hippocampal neurons: therapeutic implications. Endocrinology *147*, 5303–5313. https://doi.org/10.1210/en.2006-0495.
31. Wu, T.-W., Wang, J.M., Chen, S., and Brinton, R.D. (2005). 17β-estradiol induced Ca2+ influx via L-type calcium channels activates the Src/ERK/cyclic-AMP response element binding protein signal pathway and BCL-2 expression in rat hippocampal neurons: a potential initiation mechanism for estrogen-induced neuroprotection. Neuroscience *135*, 59–72.
32. Yao, J., Zhao, L., Mao, Z., Chen, S., Wong, K.C., To, J., and Brinton, R.D. (2013). Potentiation of brain mitochondrial function by S-equol and R/S-equol estrogen receptor beta-selective phytoSERM treatments. Brain Res. *1514*, 128–141. https://doi.org/10.1016/j.brainres.2013.02.021.
33. Zhao, L., Mao, Z., Schneider, L.S., and Brinton, R.D. (2011). Estrogen receptor beta-selective phytoestrogenic formulation prevents physical and neurological changes in a preclinical model of human menopause. Menopause *18*, 1131–1142. https://doi.org/10.1097/gme.0b013e3182175b66.
34. Zhao, L., O'Neill, K., and Brinton, R.D. (2006). Estrogenic agonist activity of ICI 182,780 (Faslodex) in hippocampal neurons: implications for basic science understanding of estrogen signaling and development of estrogen modulators with a dual therapeutic profile. J. Pharmacol. Exp. Ther. *319*, 1124–1132. https://doi.org/10.1124/jpet.106.109504.
35. Irwin, R.W., Yao, J., To, J., Hamilton, R.T., Cadenas, E., and Brinton, R.D. (2012). Selective oestrogen receptor modulators differentially potentiate brain mitochondrial function. J. Neuroendocrinol. *24*, 236–248. https://doi.org/10.1111/j.1365-2826.2011.02251.x.
36. Brinton, R.D. (2009). Estrogen-induced plasticity from cells to circuits: predictions for cognitive function. Trends Pharmacol. Sci. *30*, 212–222. https://doi.org/10.1016/j.tips.2008.12.006.
37. Foy, M.R., Xu, J., Xie, X., Brinton, R.D., Thompson, R.F., and Berger, T.W. (1999). 17β-estradiol enhances NMDA receptor-mediated EPSPs and long-term potentiation. J. Neurophysiol. *81*, 925–929.
38. Kim, M.T., Soussou, W., Gholmieh, G., Ahuja, A., Tanguay, A., Berger, T.W., and Brinton, R.D. (2006). 17β-estradiol potentiates field excitatory postsynaptic potentials within each subfield of the hippocampus with greatest potentiation of the associational/commissural afferents of CA3. Neuroscience *141*, 391–406.
39. Woolley, C.S. (2007). Acute effects of estrogen on neuronal physiology. Annu. Rev. Pharmacol. Toxicol. *47*, 657–680. https://doi.org/10.1146/annurev.pharmtox.47.120505.105219.
40. Reich, D.S., Mechler, F., Purpura, K.P., and Victor, J.D. (2000). Interspike Intervals, Receptive Fields, and Information Encoding in Primary Visual Cortex. J. Neurosci. *20*, 1964–1974. https://doi.org/10.1523/JNEUROSCI.20-05-01964.2000.
41. Ding, F., Yao, J., Rettberg, J.R., Chen, S., and Brinton, R.D. (2013). Early decline in glucose transport and metabolism precedes shift to ketogenic system in female aging and Alzheimer's mouse brain: implication for bioenergetic intervention. PLoS One *8*, e79977. https://doi.org/10.1371/journal.pone.0079977.
42. Mosconi, L., Berti, V., Quinn, C., McHugh, P., Petrongolo, G., Osorio, R.S., Connaughty, C., Pupi, A., Vallabhajosula, S., Isaacson, R.S., et al. (2017). Perimenopause and emergence of an Alzheimer's bioenergetic phenotype in brain and periphery. PLoS One *12*, e0185926. https://doi.org/10.1371/journal.pone.0185926.
43. Rettberg, J.R., Yao, J., and Brinton, R.D. (2014). Estrogen: a master regulator of bioenergetic systems in the brain and body. Front. Neuroendocrinol. *35*, 8–30. https://doi.org/10.1016/j.yfrne.2013.08.001.
44. Yao, J., and Brinton, R.D. (2012). Estrogen regulation of mitochondrial bioenergetics: implications for prevention of Alzheimer's disease. Adv. Pharmacol. *64*, 327–371. https://doi.org/10.1016/B978-0-12-394816-8.00010-6.
45. Yao, J., Irwin, R.W., Zhao, L., Nilsen, J., Hamilton, R.T., and Brinton, R.D. (2009). Mitochondrial bioenergetic deficit precedes Alzheimer's pathology in female mouse model of Alzheimer's disease. Proc. Natl. Acad. Sci. USA. *106*, 14670–14675. https://doi.org/10.1073/pnas.0903563106.
46. Yin, F., Yao, J., Sancheti, H., Feng, T., Melcangi, R.C., Morgan, T.E., Finch, C.E., Pike, C.J., Mack, W.J., Cadenas, E., and Brinton, R.D. (2015). The perimenopausal aging transition in the female rat brain: decline in bioenergetic systems and synaptic plasticity. Neurobiol. Aging *36*, 2282–2295. https://doi.org/10.1016/j.neurobiolaging.2015.03.013.
47. Brinton, R.D., Yao, J., Yin, F., Mack, W.J., and Cadenas, E. (2015). Perimenopause as a neurological transition state. Nat. Rev. Endocrinol. *11*, 393–405. https://doi.org/10.1038/nrendo.2015.82.
48. Alliot, C. (2005). Undertreatment of Breast Cancer in Elderly Women: Contribution of a Cancer Registry. J. Clin. Oncol. *23*, 4800–4801. author reply 4801-4802. https://doi.org/10.1200/jco.2005.01.4241.

49. (2020). 2020 Alzheimer's Disease Facts and Figures. Alzheimers Dement. https://doi.org/10.1002/alz.12068.
50. Henderson, V.W., Ala, T., Sainani, K.L., Bernstein, A.L., Stephenson, B.S., Rosen, A.C., and Farlow, M.R. (2015). Raloxifene for women with Alzheimer disease: A randomized controlled pilot trial. Neurology *85*, 1937–1944. https://doi.org/10.1212/wnl.0000000000002171.
51. Liao, K.F., Lin, C.L., and Lai, S.W. (2017). Nationwide Case-Control Study Examining the Association between Tamoxifen Use and Alzheimer's Disease in Aged Women with Breast Cancer in Taiwan. Front. Pharmacol. *8*, 612. https://doi.org/10.3389/fphar.2017.00612.
52. Sun, L.M., Chen, H.J., Liang, J.A., and Kao, C.H. (2016). Long-term use of tamoxifen reduces the risk of dementia: a nationwide population-based cohort study. QJM *109*, 103–109. https://doi.org/10.1093/qjmed/hcv072.
53. Thompson, M.R., Niu, J., Lei, X., Nowakowska, M., Wehner, M.R., Giordano, S.H., and Nead, K.T. (2021). Association of Endocrine Therapy and Dementia in Women with Breast Cancer. Breast Cancer (Dove Med Press) *13*, 219–224. https://doi.org/10.2147/bctt.S300455.
54. Kim, Y.J., Soto, M., Branigan, G.L., Rodgers, K., and Brinton, R.D. (2021). Association between menopausal hormone therapy and risk of neurodegenerative diseases: Implications for precision hormone therapy. Alzheimers Dement. *7*, e12174. https://doi.org/10.1002/trc2.12174.
55. Kim, Y.J., and Brinton, R.D. (2021). Precision hormone therapy: identification of positive responders. Climacteric *24*, 350–358. https://doi.org/10.1080/13697137.2021.1882418.
56. Yaffe, K., Krueger, K., Cummings, S.R., Blackwell, T., Henderson, V.W., Sarkar, S., Ensrud, K., and Grady, D. (2005). Effect of raloxifene on prevention of dementia and cognitive impairment in older women: the Multiple Outcomes of Raloxifene Evaluation (MORE) randomized trial. Am. J. Psychiatry *162*, 683–690. https://doi.org/10.1176/appi.ajp.162.4.683.
57. Yaffe, K., Krueger, K., Sarkar, S., Grady, D., Barrett-Connor, E., Cox, D.A., and Nickelsen, T.; Multiple Outcomes of Raloxifene Evaluation Investigators (2001). Cognitive function in postmenopausal women treated with raloxifene. N. Engl. J. Med. *344*, 1207–1213. https://doi.org/10.1056/nejm200104193441604.
58. Kara, F., Lohse, C.M., Castillo, A.M., Tosakulwong, N., Lesnick, T.G., Jack Jr, C.R., Petersen, R.C., Olson, J.E., Couch, F.J., Ruddy, K.J., et al. Association of Raloxifene and Tamoxifen Therapy with Cognitive Performance, Odds of Mild Cognitive Impairment, and Brain MRI Markers of Neurodegeneration. Cancer Medicine n/a. https://doi.org/10.1002/cam4.5175
59. Dutertre, M., and Smith, C.L. (2000). Molecular mechanisms of selective estrogen receptor modulator (SERM) action. J. Pharmacol. Exp. Ther. *295*, 431–437.
60. Gougelet, A., Mueller, S.O., Korach, K.S., and Renoir, J.M. (2007). Oestrogen receptors pathways to oestrogen responsive elements: the transactivation function-1 acts as the keystone of oestrogen receptor (ER)beta-mediated transcriptional repression of ERalpha. J. Steroid Biochem. Mol. Biol. *104*, 110–122. https://doi.org/10.1016/j.jsbmb.2007.03.002.
61. Légaré, S., and Basik, M. (2016). Minireview: The Link Between ERα Corepressors and Histone Deacetylases in Tamoxifen Resistance in Breast Cancer. Mol. Endocrinol. *30*, 965–976. https://doi.org/10.1210/me.2016-1072.
62. Tetel, M.J., Auger, A.P., and Charlier, T.D. (2009). Who's in charge? Nuclear receptor coactivator and corepressor function in brain and behavior. Front. Neuroendocrinol. *30*, 328–342. https://doi.org/10.1016/j.yfrne.2009.04.008.
63. Tognoni, C.M., Chadwick, J.G., Jr., Ackeifi, C.A., and Tetel, M.J. (2011). Nuclear Receptor Coactivators Are Coexpressed with Steroid Receptors and Regulated by Estradiol in Mouse Brain. Neuroendocrinology *94*, 49–57. https://doi.org/10.1159/000323780.
64. McEwen, B.S., and Alves, S.E. (1999). Estrogen actions in the central nervous system. Endocr. Rev. *20*, 279–307.
65. Ramírez-Barrantes, R., Marchant, I., and Olivero, P. (2016). TRPV1 may increase the effectiveness of estrogen therapy on neuroprotection and neuroregeneration. Neural Regen. Res. *11*, 1204–1207. https://doi.org/10.4103/1673-5374.189162.
66. Marchant, I., Stojanova, J., Acevedo, L., and Olivero, P. (2022). Estrogen rapid effects: a window of opportunity for the aging brain? Neural Regen. Res. *17*, 1629–1632. https://doi.org/10.4103/1673-5374.332121.
67. Romanò, N., Lee, K., Abrahám, I.M., Jasoni, C.L., and Herbison, A.E. (2008). Nonclassical Estrogen Modulation of Presynaptic GABA Terminals Modulates Calcium Dynamics in Gonadotropin-Releasing Hormone Neurons. Endocrinology *149*, 5335–5344. https://doi.org/10.1210/en.2008-0424.
68. Brinton, R.D. (2001). Cellular and molecular mechanisms of estrogen regulation of memory function and neuroprotection against Alzheimer's disease: recent insights and remaining challenges. Learn. Mem. *8*, 121–133.
69. Mosconi, L., Berti, V., Quinn, C., McHugh, P., Petrongolo, G., Varsavsky, I., Osorio, R.S., Pupi, A., Vallabhajosula, S., Isaacson, R.S., et al. (2017). Sex differences in Alzheimer risk: Brain imaging of endocrine vs chronologic aging. Neurology *89*, 1382–1390. https://doi.org/10.1212/wnl.0000000000004425.
70. Green, P.S., and Simpkins, J.W. (2000). Neuroprotective effects of estrogens: potential mechanisms of action. Int. J. Dev. Neurosci. *18*, 347–358.
71. Simoncini, T., Hafezi-Moghadam, A., Brazil, D.P., Ley, K., Chin, W.W., and Liao, J.K. (2000). Interaction of oestrogen receptor with the regulatory subunit of phosphatidylinositol-3-OH kinase. Nature *407*, 538–541.
72. Wymann, M.P., and Pirola, L. (1998). Structure and function of phosphoinositide 3-kinases. Biochim. Biophys. Acta *1436*, 127–150.
73. Hinkle, P.M., Nelson, E.J., and Haymes, A.A. (1993). Regulation of L-type voltage-gated calcium channels by epidermal growth factor. Endocrinology *133*, 271–276.
74. Cordey, M., Gundimeda, U., Gopalakrishna, R., and Pike, C.J. (2003). Estrogen activates protein kinase C in neurons: role in neuroprotection. J. Neurochem. *84*, 1340–1348.
75. Guo, J., Meng, F., Fu, X., Song, B., Yan, X., and Zhang, G. (2004). N-methyl-D-aspartate receptor and L-type voltage-gated Ca2+ channel activation mediate proline-rich tyrosine kinase 2 phosphorylation during cerebral ischemia in rats. Neurosci. Lett. *355*, 177–180.
76. Migliaccio, A., Di Domenico, M., Castoria, G., de Falco, A., Bontempo, P., Nola, E., and Auricchio, F. (1996). Tyrosine kinase/p21ras/MAP-kinase pathway activation by estradiol-receptor complex in MCF-7 cells. The EMBO journal *15*, 1292–1300.
77. Nilsen, J., and Brinton, R.D. (2002). Impact of progestins on estrogen-induced neuroprotection: synergy by progesterone and 19-norprogesterone and antagonism by medroxyprogesterone acetate. Endocrinology *143*, 205–212.
78. Nilsen, J., Chen, S., and Brinton, R.D. (2002). Dual action of estrogen on glutamate-induced calcium signaling: mechanisms requiring interaction between estrogen receptors and src/mitogen activated protein kinase pathway. Brain Res. *930*, 216–234.
79. López-González, I., Schlüter, A., Aso, E., Garcia-Esparcia, P., Ansoleaga, B., LLorens, F., Carmona, M., Moreno, J., Fuso, A., Portero-Otin, M., et al. (2015). Neuroinflammatory signals in Alzheimer disease and APP/PS1 transgenic mice: correlations with plaques, tangles, and oligomeric species. J. Neuropathol. Exp. Neurol. *74*, 319–344. https://doi.org/10.1097/nen.0000000000000176.
80. Kuiper, G.G., Carlsson, B., Grandien, K., Enmark, E., Häggblad, J., Nilsson, S., and Gustafsson, J.A. (1997). Comparison of the ligand binding specificity and transcript tissue distribution of estrogen receptors alpha and beta. Endocrinology *138*, 863–870. https://doi.org/10.1210/endo.138.3.4979.
81. Paech, K., Webb, P., Kuiper, G.G., Nilsson, S., Gustafsson, J., Kushner, P.J., and Scanlan, T.S. (1997). Differential ligand activation of estrogen receptors ERalpha and ERbeta at AP1 sites. Science *277*, 1508–1510. https://doi.org/10.1126/science.277.5331.1508.
82. McEwen, B.S., Akama, K.T., Spencer-Segal, J.L., Milner, T.A., and Waters, E.M. (2012). Estrogen effects on the brain: actions beyond the hypothalamus via novel mechanisms. Behav. Neurosci. *126*, 4–16. https://doi.org/10.1037/a0026708.
83. McEwen, B.S. (1999). The Molecular and Neuroanatomical Basis for Estrogen Effects in the Central Nervous System. J. Clin. Endocrinol. Metab. *84*, 1790–1797. https://doi.org/10.1210/jcem.84.6.5761.
84. Srinivasan, R., Lu, T.Y., Chai, H., Xu, J., Huang, B.S., Golshani, P., Coppola, G., and Khakh, B.S. (2016). New Transgenic Mouse Lines for Selectively Targeting Astrocytes and Studying Calcium Signals in Astrocyte Processes In Situ and In Vivo. Neuron *92*, 1181–1195. https://doi.org/10.1016/j.neuron.2016.11.030.
85. Nagai, M.A., and Brentani, M.M. (2008). Gene expression profiles in breast cancer to identify estrogen receptor target genes. Mini Rev. Med. Chem. *8*, 448–454. https://doi.org/10.2174/138955708784223503.
86. Lee, C.M., Zhou, L., Liu, J., Shi, J., Geng, Y., Liu, M., Wang, J., Su, X., Barad, N., Wang, J., et al. (2020). Single-cell RNA-seq analysis revealed long-lasting adverse effects of

tamoxifen on neurogenesis in prenatal and adult brains. Proc. Natl. Acad. Sci. USA. *117*, 19578–19589. https://doi.org/10.1073/pnas.1918883117.

87. Galvano, E., Pandit, H., Sepulveda, J., Ng, C.A.S., Becher, M.K., Mandelblatt, J.S., Van Dyk, K., and Rebeck, G.W. (2023). Behavioral and transcriptomic effects of the cancer treatment tamoxifen in mice. Front. Neurosci. *17*, 1068334. https://doi.org/10.3389/fnins.2023.1068334.
88. Chucair-Elliott, A.J., Ocanas, S.R., Stanford, D.R., Hadad, N., Wronowski, B., Otalora, L., Stout, M.B., and Freeman, W.M. (2019). Tamoxifen induction of Cre recombinase does not cause long-lasting or sexually divergent responses in the CNS epigenome or transcriptome: implications for the design of aging studies. Geroscience *41*, 691–708. https://doi.org/10.1007/s11357-019-00090-2.
89. Scharfman, H.E., Malthankar-Phatak, G.H., Friedman, D., Pearce, P., McCloskey, D.P., Harden, C.L., and Maclusky, N.J. (2009). A rat model of epilepsy in women: a tool to study physiological interactions between endocrine systems and seizures. Endocrinology *150*, 4437–4442. https://doi.org/10.1210/en.2009-0135.
90. Scharfman, H.E. (2005). The Absence of Information about Hormones and Absence. Epilepsy Curr. *5*, 101–103. https://doi.org/10.1111/j.1535-7511.2005.05309.x.
91. Finney, C.A., Shvetcov, A., Westbrook, R.F., Morris, M.J., and Jones, N.M. (2021). The selective estrogen receptor modulator tamoxifen protects against subtle cognitive decline and early markers of injury 24 h after hippocampal silent infarct in male Sprague-Dawley rats. Horm. Behav. *134*, 105016. https://doi.org/10.1016/j.yhbeh.2021.105016.
92. Smith, B.M., Saulsbery, A.I., Sarchet, P., Devasthali, N., Einstein, D., and Kirby, E.D. (2022). Oral and Injected Tamoxifen Alter Adult Hippocampal Neurogenesis in Female and Male Mice. eNeuro *9*. ENEURO.0422, 21.2022. https://doi.org/10.1523/eneuro.0422-21.2022.
93. Klann, I.P., Fulco, B.C.W., and Nogueira, C.W. (2023). Subchronic exposure to Tamoxifen modulates the hippocampal BDNF/ERK/Akt/CREB pathway and impairs memory in intact female rats. Chem. Biol. Interact. *382*, 110615. https://doi.org/10.1016/j.cbi.2023.110615.
94. Soldati, C., Lopez-Fabuel, I., Wanderlingh, L.G., Garcia-Macia, M., Monfregola, J., Esposito, A., Napolitano, G., Guevara-Ferrer, M., Scotto Rosato, A., Krogsaeter, E.K., et al. (2021). Repurposing of tamoxifen ameliorates CLN3 and CLN7 disease phenotype. EMBO Mol. Med. *13*, e13742. https://doi.org/10.15252/emmm.202013742.
95. Norton, S., Matthews, F.E., Barnes, D.E., Yaffe, K., and Brayne, C. (2014). Potential for primary prevention of Alzheimer's disease: an analysis of population-based data. Lancet Neurol. *13*, 788–794. https://doi.org/10.1016/s1474-4422(14)70136-x.
96. Pareto, D., Alvarado, M., Hanrahan, S.M., and Biegon, A. (2004). In vivo occupancy of female rat brain estrogen receptors by 17beta-estradiol and tamoxifen. Neuroimage *23*, 1161–1167. https://doi.org/10.1016/j.neuroimage.2004.07.036.
97. Lien, E.A., Solheim, E., and Ueland, P.M. (1991). Distribution of tamoxifen and its metabolites in rat and human tissues during steady-state treatment. Cancer Res. *51*, 4837–4844.
98. Pourreau-Schneider, N., Berthois, Y., Gandilhon, P., Cau, P., and Martin, P.M. (1986). Early alterations at the plasma membrane of breast cancer cell lines in response to estradiol and hydroxytamoxifen. Mol. Cell. Endocrinol. *48*, 77–88. https://doi.org/10.1016/0303-7207(86)90168-1.
99. Ribeiro, M., Elghajiji, A., Fraser, S.P., Burke, Z.D., Tosh, D., Djamgoz, M.B.A., and Rocha, P.R.F. (2020). Human Breast Cancer Cells Demonstrate Electrical Excitability. Front. Neurosci. *14*, 404. https://doi.org/10.3389/fnins.2020.00404.
100. Ruffy, M.B., Kunnavatana, S.S., and Koch, R.J. (2006). Effects of tamoxifen on normal human dermal fibroblasts. Arch. Facial Plast. Surg. *8*, 329–332. https://doi.org/10.1001/archfaci.8.5.329.
101. Lattrich, C., Schüler, S., Häring, J., Skrzypczak, M., Ortmann, O., and Treeck, O. (2014). Effects of a combined treatment with tamoxifen and estrogen receptor β agonists on human breast cancer cell lines. Arch. Gynecol. Obstet. *289*, 163–171. https://doi.org/10.1007/s00404-013-2977-7.
102. Aisen, P.S., Cummings, J., Jack, C.R., Jr., Morris, J.C., Sperling, R., Frölich, L., Jones, R.W., Dowsett, S.A., Matthews, B.R., Raskin, J., et al. (2017). On the path to 2025: understanding the Alzheimer's disease continuum. Alzheimer's Res. Ther. *9*, 60. https://doi.org/10.1186/s13195-017-0283-5.
103. Matsen, C.B., and Neumayer, L.A. (2013). Breast cancer: a review for the general surgeon. JAMA Surg. *148*, 971–979. https://doi.org/10.1001/jamasurg.2013.3393.
104. Torrandell-Haro, G., Branigan, G.L., Vitali, F., Geifman, N., Zissimopoulos, J.M., and Brinton, R.D. (2020). Statin therapy and risk of Alzheimer's and age-related neurodegenerative diseases. Alzheimers Dement. *6*, e12108. https://doi.org/10.1002/trc2.12108.
105. Yao, J., Irwin, R., Chen, S., Hamilton, R., Cadenas, E., and Brinton, R.D. (2012). Ovarian hormone loss induces bioenergetic deficits and mitochondrial beta-amyloid. Neurobiol. Aging *33*, 1507–1521. https://doi.org/10.1016/j.neurobiolaging.2011.03.001.
106. Qi, G., Mi, Y., Shi, X., Gu, H., Brinton, R.D., and Yin, F. (2021). ApoE4 Impairs Neuron-Astrocyte Coupling of Fatty Acid Metabolism. Cell Rep. *34*, 108572. https://doi.org/10.1016/j.celrep.2020.108572.
107. Nilsen, J., Chen, S., Irwin, R.W., Iwamoto, S., and Brinton, R.D. (2006). Estrogen protects neuronal cells from amyloid beta-induced apoptosis via regulation of mitochondrial proteins and function. BMC Neurosci. *7*, 74.
108. Phillips, C., Roberts, L.R., Schade, M., Bazin, R., Bent, A., Davies, N.L., Moore, R., Pannifer, A.D., Pickford, A.R., Prior, S.H., et al. (2011). Design and structure of stapled peptides binding to estrogen receptors. J. Am. Chem. Soc. *133*, 9696–9699. https://doi.org/10.1021/ja202946k.
109. Möcklinghoff, S., Rose, R., Carraz, M., Visser, A., Ottmann, C., and Brunsveld, L. (2010). Synthesis and crystal structure of a phosphorylated estrogen receptor ligand binding domain. Chembiochem *11*, 2251–2254. https://doi.org/10.1002/cbic.201000532.
110. Henke, B.R., Consler, T.G., Go, N., Hale, R.L., Hohman, D.R., Jones, S.A., Lu, A.T., Moore, L.B., Moore, J.T., Orband-Miller, L.A., et al. (2002). A new series of estrogen receptor modulators that display selectivity for estrogen receptor beta. J. Med. Chem. *45*, 5492–5505. https://doi.org/10.1021/jm020291h.
111. Sastry, G.M., Adzhigirey, M., Day, T., Annabhimoju, R., and Sherman, W. (2013). Protein and ligand preparation: parameters, protocols, and influence on virtual screening enrichments. J. Comput. Aided Mol. Des. *27*, 221–234. https://doi.org/10.1007/s10822-013-9644-8.
112. Schrödinger Release 2020-4 (2020 (Schrödinger, LLC).
113. Friesner, R.A., Banks, J.L., Murphy, R.B., Halgren, T.A., Klicic, J.J., Mainz, D.T., Repasky, M.P., Knoll, E.H., Shelley, M., Perry, J.K., et al. (2004). Glide: a new approach for rapid, accurate docking and scoring. 1. Method and assessment of docking accuracy. J. Med. Chem. *47*, 1739–1749. https://doi.org/10.1021/jm0306430.
114. Bell, E.W., and Zhang, Y. (2019). DockRMSD: an open-source tool for atom mapping and RMSD calculation of symmetric molecules through graph isomorphism. J. Cheminform. *11*, 40. https://doi.org/10.1186/s13321-019-0362-7.
115. The PyMOL Molecular Graphics System, Version 2.0 Schrödinger, LLC.
116. Patro, R., Duggal, G., Love, M.I., Irizarry, R.A., and Kingsford, C. (2017). Salmon provides fast and bias-aware quantification of transcript expression. Nat. Methods *14*, 417–419. https://doi.org/10.1038/nmeth.4197.
117. Love, M.I., Huber, W., and Anders, S. (2014). Moderated estimation of fold change and dispersion for RNA-seq data with DESeq2. Genome Biol. *15*, 550. https://doi.org/10.1186/s13059-014-0550-8.
118. Soneson, C., Love, M., and Robinson, M. (2015). Differential analyses for RNA-seq: transcript-level estimates improve gene-level inferences [version 1; peer review: 2 approved]. F1000Research *4*. https://doi.org/10.12688/f1000research.7563.1.

STAR★METHODS

KEY RESOURCES TABLE

REAGENT or RESOURCE	SOURCE	IDENTIFIER
Antibodies		
Anti-MAP-2	Sigma	M4403; RRID: AB_477193
TOM20	ThermoFisher	PA5-52843; RRID: AB_2648808
Chemicals, peptides, and recombinant proteins		
B-27 supplement	Gibco	17504044
L-glutamine	Gibco	25030081
phenol red–free Neurobasal medium	Gibco	12348017
Glutamate	MP Biomedicals	02101800
penicillin/streptomycin	Gibco	15140122
estradiol E2	Sigma	1250008
tamoxifen	Sigma	85256
raloxifene	Sigma	1598201
anastrozole	Sigma	1034807
exemestane	Sigma	1269050
TaqMan™ Universal PCR Master Mix	Applied Biosystems	4304437
GlutaMAX	Gibco	35050061
oligomycin	MP Biomedicals	02151786
FCCP	TOCRIS Bioscience	0453
rotenone	MP Biomedicals	02150154
antimycin	Sigma-Aldrich	A-8674
Critical commercial assays		
TaqMan® Array 96-well Human Estrogens Plates	ThermoScientific	4418732
TaqMan® Array Rat 96-well Estrogen Signaling Plates	ThermoScientific	4413255
SuperScript VILO cDNA Synthesis Kit	ThermoScientific	11754050
Deposited data		
RNAseq data	GEO	GSE241054
Experimental models: Organisms/strains		
Sprague Dawley rat	Charles River	Crl:CD(SD)
Software and algorithms		
Imaris 9.3.0 software	Oxford Instruments	N/A
Schrödinger Release 2020-4	Schrödinger, LLC	N/A
Salmon 1.5.2	R studio	N/A
DESeq2	R studio	N/A
Tximport	R studio	N/A
IPA- Ingenuity Pathway Analysis	QIAGEN	N/A
Other		
Laser-Scanning Microscopy	Zeiss	N/A
Multi-electrode array	Alpha Med Scientific	N/A
XF96e metabolic flus analyzer	Agilent	N/A
QuantStudio™ 12K Flex system	Applied Biosystems	N/A

RESOURCE AVAILABILITY

Lead contact

Further information and requests for data, reagents, or resources should be directed to and will be fulfilled by the lead contact, Roberta Diaz Brinton (rbrinton@arizona.edu).

Materials availability

This study did not generate new unique reagents.

Data and code availability

- Single-cell RNA-seq data have been deposited at GEO and are publicly available as of the date of publication. Accession numbers are listed in the key resources table.
- Restrictions apply to the availability of the code generated or analyzed during this study to preserve patient confidentiality or because they were used under license. The corresponding author will on request detail the restrictions and any conditions under which access to some data may be provided.
- Any additional information required to reanalyze the data reported in this paper is available from the lead contact upon request.

EXPERIMENTAL MODEL AND STUDY PARTICIPANT DETAILS

40 female Sprague Dawley rats were obtained from Charles River Laboratories. The animals were acclimatized to standard laboratory conditions (temperature 22°C–25°C, relative humidity 50-60%, and 12-hour photoperiods (lights on 07:00-19:00)) and were housed in stainless steel wire-mesh cages (3 rats per cage). During the entire period of study, the rats were supplied with a semipurified basal diet and water *ad libitum*. All experiments followed the Guide for the Care and Use of Laboratory Animals. Rats were ovariectomized at 6 months of age at Charles River Laboratories. After a 2-week wash-out period, rats were treated (see EMT treatment).

All animal studies were performed following National Institutes of Health guidelines on use of laboratory animals and all protocols were approved by the University of Arizona Institutional Animal Care and Use Committee.

METHOD DETAILS

Medical informatics: Data source

The Mariner database is an insurance claims dataset that serves the United States with patient populations from all U.S. states and territories. Pearl Diver is for-fee research software that facilitates interaction with individual commercial, state-based Medicaid, Medicare stand-alone prescription drug plan, group Medicare Advantage, and individual Medicare Advantage data. The Mariner dataset contains patient demographic characteristics, prescription records, and numerous other data points for patients with *Current Procedural Terminology*, *International Classification of Diseases, Ninth Revision (ICD-9)*, and *International Statistical Classification of Diseases and Related Health Problems, Tenth Revision (ICD-10)* codes. As of October 2020, Mariner encompasses all indications and represents 122 million patients throughout the duration of the set with claims from 2010 through the second quarter of 2018.

This report follows the Strengthening the Reporting of Observational Studies in Epidemiology (STROBE) reporting guideline. This study was approved by the University of Arizona Institutional Review Board. Requirements for informed consent were waived as the data were deidentified.

Medical informatics: Study design and variables

The outcome variable was defined as the occurrence of the first diagnosis of Alzheimer's disease (AD based on ICD-9 and ICD-10 codes in the patient's medical claims data (Table S3). An index date one year after the diagnosis of breast cancer was selected to allow for onboarding to therapy and to focus on long-term impact on disease progression given the prodromal nature of these neurodegenerative diseases. Participants younger than 45 years old, with a diagnosis of other cancers, or with a history of neurosurgery, brain cancer, or neurodegenerative disease prior to the index date were excluded from the study. An enrollment criterion in the claims dataset of at least 6 months prior to and 3 years after the diagnosis of breast cancer was applied. The enrollment criteria was required before any analysis of exposure to EMT for development of AD for all patients to account for patients that may be leaving, dying, or switching the insurance provider (Figure 1A). Additionally, the 3-year follow-up is not with respect to EMT exposure but instead with respect to breast cancer diagnosis. Patient groups were defined according to the therapeutic intervention used. The treatment group is defined as patients having at least one medication charge for an EMT agent occurring after the diagnosis of breast cancer. This group was then stratified based on the mechanism of action of each therapeutic intervention for EMT (Table S1). The EMT group was defined as patients with one or more codes for tamoxifen, raloxifene, fluvestrant, letrozole, anastrozole, or exemestane (Table S1). Drug groups with a low number of patients were not included in the sensitivity analysis evaluating the association between AD and individual drug groups but were included in the relative risk analysis of overall EMT. Median adherence rates for each drug as well as the duration of treatment are reported in Table S1. Age in the study is defined by the age at diagnosis of breast cancer. An analysis of comorbidities known to be associated with AD outcomes was conducted (Table S2) which was used to generate a logistic regression-based propensity score matched cohort for treatment and control populations.

Medical informatics: Statistical analysis

Statistical analyses were conducted between January 1st and February 2th, 2022. Patient demographic statistics and incidence statistics were analyzed using unpaired 2-tailed t-tests or $\chi 2$ tests, as appropriate, to test the significance of the differences between continuous and categorical variables. In all analyses, a 2-sided $P < 0.05$ was considered statistically significant.

A propensity score-matched population was generated by using a logistic regression to identify confounding factors for therapeutic treatment of breast cancer as outcome between the treatment and control groups as previously reported.[18,104] In brief, the resulting factors included age, region, gender, Charlson Comorbidity Index (CCI) rank as well as variable comorbidities including Asthma, Chronic Obstructive Pulmonary Disease (COPD), Chronic Kidney Disease, Congestive Heart Failure, Coronary Artery Disease, Hypertension, Obesity, Pulmonary Heart Disease, Ischemic Heart Disease, Tobacco Use, Osteoarthritis, Rheumatoid Arthritis, Stroke and Tobacco Use (Table S3). These factors were then used to match patients in the treatment group to patients in the control group to minimize confounding variables in the patient populations. The matching was assessed by standardized mean difference with percentage balance improvement. Kaplan-Meier survival curves for AD-Free Survival were created using the propensity score-matched population in the Bellwether-PearlDiver interface.

Animal use

All animal studies were performed following National Institutes of Health guidelines on use of laboratory animals and all protocols were approved by the University of Arizona Institutional Animal Care and Use Committee.

Cell culture

Primary neurons

Hippocampal neurons were isolated from Sprague Dawley rat embryos at day 18 (E18). Briefly, hippocampi were dissected from the brains of embryonic day 18 fetuses. Hippocampal tissues were dissociated by incubation with 0.02% trypsin in HBSS (5.4mM KCl, 137mM NaCl, 0.4mM KH2PO4, 0.34mM Na2HPO4x7H2O, 10mM glucose, and 10mM HEPES) for 3 min at 37C and repeated passage through a series of fire-polished constricted Pasteur pipettes. Cell suspension was filtered through 40 mm Nylon cell strainer into 50 mL conical centrifuge tubes and centrifuged at 1,000 rpm for 3min. Neurons were cultured in poly-D-lysine coated culture vessels, with phenol red–free Neurobasal medium (Gibco, 12348017), supplemented with 2% B-27 (Gibco, 17504044), 0.5mM L-glutamine (Gibco, 25030081), 25uM glutamate (MP Biomedicals, 02101800), and 10U/mL penicillin/streptomycin (Gibco, 15140122). On *in vitro* day 4, glutamate was removed from culture medium. On *in vitro* day 10, neurons were treated with desired reagents, and downstream assays were performed on *in vitro* day 11.

In vitro treatment

To test for the effect of estradiol, cells were treated with either vehicle (EtOH equally diluted to 10ng/mL), estradiol E2 (10ng/mL), tamoxifen (10ng/mL), raloxifene (1pg/mL), anastrozole (5ng/mL), or exemestane (10ng/mL) for 24 hours before downstream experiments. These concentrations were determined based on steady-state concentration in human plasma,[22–25] previous experiments[8,9,26–34] and functional assay outcomes.[35]

Morphological analysis

Immunostaining and confocal imaging were used to determine neuronal morphological characteristics. Cells cultured on coverslips were fixed with 4% paraformaldehyde in PBS for 15 min, rinsed with PBS for 3 times and incubated in blocking buffer (5% normal goat serum + 0.3% Triton X-100 in PBS) for 1h at room temperature. Anti-MAP-2 (1:1000, Sigma, M4403) primary antibody (diluted in blocking buffer) staining was performed overnight at 4C. Secondary antibody (Alexa Fluor 488 goat anti-mouse, 1:1000, Invitrogen) staining was conducted at room temperature for 1h. Coverslips were mounted with mounting medium containing DAPI on slides and sealed with nail polish after cleaning the edge. Images were captured with Zeiss Laser-Scanning Microscopy (LSM) 880 with Airyscan detector using 10X objective lens or 20X objective lens. Quantification of neurite length, branch, and area was performed using Imaris 9.3.0 software. Each data point represents the averaged value of all cells on a coverslip.

Electrophysiological recordings

Rat primary neurons were cultured at a density of 3.0 x 10^5 cells/cm^2 in the center of a multi-electrode array (MEA) containing 16 Indium-Tin Oxide recording electrodes that are coated with polyethyleneimine and laminin-511 to promote neuronal attachment (Alpha Med Scientific, Osaka Japan). Half of the culture medium was replaced every 3 days until the cells were ready for recording at culture day 12. Coverage of the MEA recording sites with neurons was confirmed using an inverted microscope after 5 days in culture. Recordings of spontaneous firing activity was captured at all 16 electrodes simultaneously with well temperature maintained at 37C and a 95% O2 and 5% CO2 gas mixture during the entire recording period. To identify neuronal spiking events, signals are bandpass filtered with a high-pass setting of 100 Hz and a low-pass value of 3 kHz. To identify spike events correlated with neuronal firing, a threshold-based method was applied where a spike was considered if it crosses a threshold equal to 4x the standard deviation of the RMS baseline noise. Once a spike crosses the threshold, a window capturing 1.5ms before and 2.5ms after the crossing event was extracted from the recording and stored as a separate data file comprising all detected spikes. This extracted spike-time data was analyzed using k-means clustering to identify groups of spikes that are attributed to a single neuron. A neuron burst was defined by greater than 20 spikes/ms.

Metabolic flux assay

Cellular respiratory capacity was determined by XF96e metabolic flus analyzer as previously described.[32,35,44,45,105,106] Briefly, cells were seeded into appropriately coated cell plates at desired density (50,000/well for primary neurons), cultured and treated as described above. On the day of assay, culture medium was changed to unbuffered DMEM (Sigma-Aldrich, D5030) medium supplemented with 25mM glucose, 1mM sodium pyruvate, and 2mM GlutaMAX for primary cells (Gibco, 35050061). Medium pH was adjusted to 7.4. Cells were incubated at 37°C in a non-CO2 incubator for 1 hour. Oxygen consumption rate (OCR) was used as an indicator of mitochondrial oxidative phosphorylation, and mitochondrial basal respiration, ATP production, maximal respiratory capacity, and proton leak were determined by sequential acute injection of mitochondrial electron transport chain inhibitors and un-couplers: oligomycin (MP Biomedicals, 02151786), FCCP (carbonyl cyanide4 (trifluoromethoxy)- phenylhydrazone) (TOCRIS Bioscience, 0453), rotenone (MP Biomedicals, 02150154), and antimycin (Sigma-Aldrich, A-8674).

For primary neurons, 4uM oligomycin, 1uM FCCP, and 1uM rotenone/antimycin were used. Results were normalized to protein reading of each plate to eliminate variation due to cell seeding and loss during assay procedures. The basal respiration was calculated as the differences between OCR before oligomycin injection and OCR after rotenone/antimycin A injection (non-mitochondrial respiration). Maximal respiration was the differences between maximal OCR value after FCCP injection and OCR after rotenone/antimycin A injection. Spare capacity ratio (SCR) is defined as the ratio of maximal respiration to basal respiration, as an indicator for the utilization of the cells' maximum bioenergetic capacity. Experiments from cells isolated from at least three animals were performed in these assays. For each animal or cell batch, there were 16-20 wells per group and 25,000 cells/well for 96-well platform. Data shown are representative result from at least 3 independent batches of cells.

In-vitro mitochondrial imaging

Immunostaining and confocal imaging were used to determined neuronal mitochondrial characteristics as previously described.[106,107] For mitochondrial labeling, Cells cultured on coverslips were fixed with 4% paraformaldehyde in PBS for 15 minutes, rinsed with PBS for 3 times and incubated in blocking buffer (5% normal goat serum + 0.3% Triton X-100 in PBS) for 1h at room temperature. Anti-TOM20 (1:250, ThermoFisher, PA5-52843) primary antibody (diluted in blocking buffer) staining was performed overnight at 4C. Secondary antibody (Alexa Fluor 488 goat anti-rabbit, 1:500, Invitrogen) staining was conducted at room temperature for 1h.

Coverslips were mounted with mounting medium containing DAPI on slides and sealed with nail polish after cleaning the edge. Images were captured with Zeiss Laser-Scanning Microscopy (LSM) 880 with Airyscan detector using 60X objective lens or 40X objective lens. Quantification of mitochondrial shape was performed using Imaris 9.3.0 software. For each treatment group, 15 cells on average were used for mitochondrial quantification and data are normalized to cell volume for the volumetric analysis per 100um.

Computation molecular modeling and docking of SERMs and estrogen receptors

Structures of the ligand binding domain of human ERα and ERβ in the antagonist and agonist-bound states were selected for docking studies as follows: ERα at 1.8 Å with estrogen E2 bound (PDB ID: 2YJA[108]) and at 1.9 Å with 4-hydroxy tamoxifen (4-OHT) bound (PDB ID: 3ERT[20]); ERβ at 2.2 Å with estrogen E2 bound (PDB ID: 3OLS[109]), and at 3.0 Å with a triazine antagonist bound (PDB ID: 1NDE[110]).

Protein targets were prepared using the Protein Preparation Wizard[111] and ligands (estrogen E2, 4-OH tamoxifen, raloxifene, exemestane, anastrozole (Figure 1A) and the triazine antagonist bound to PDB ID 1NDE[110] (as redocking control) were prepared using LigPrep with ionization states at pH 7.0. Docking studies were performed using the Schrödinger small molecule discovery suite[112] (Schrödinger Release 2020-4: Schrödinger, LLC, New York, NY, 2020) with Glide in Extra Precision (XP) mode.[113] The best of two poses was selected for analysis and figures. As controls, crystallized ligands were also prepared and docked using the same approach. The docking poses for E2 were indistinguishable from the co-crystallized conformations with all-atom root-mean square deviations (RMSD) of 0.31 Å for ERα (2YJA[108]) and 0.17 Å for ERβ (3OLS[109]). In the open state structures, 4-OHT docked with a slightly higher RMSD of 1.2 Å compared to the crystallized conformation (3ERT[20]) due to rotations at the dimethylamino linkage. The triazine antagonist docked with a score of -14.1 kcal/mole with an RMSD of 0.76 Å to the crystallized conformation (1NDE,[110] not shown). Ligand RMSD calculations were obtained through the DockRMSD web server.[114] Molecular figures were generated with PyMOL.[115]

Structures of the ligand binding domain of human ERα and ERβ in the closed (antagonist) and open (agonist) states were selected for docking studies as follows: ERα at 1.8 Å with estrogen E2 bound (PDB ID: 2YJA[108]) and at 1.9 Å with 4-hydroxy tamoxifen (4-OHT) bound (PDB ID: 3ERT[20]); ERβ at 2.2 Å with estrogen E2 bound (PDB ID: 3OLS[109]), and at 3.0 Å with a triazine antagonist bound (PDB ID: 1NDE[110]).

In-vivo EMT treatment

Rats were randomly distributed into 8 equal groups based on treatment type. Each rat was then treated according to their assignment group (i.e., sham, OVX-, OVX+EMT) at clinically relevant concentrations based on allometric dose scaling (Human Equivalent Dose Conversion [mg/kg]). The resulting dosing regimen was once daily IP injections of estradiol E2 (0.16mg/kg), tamoxifen (3.23mg/kg), raloxifene (9.68mg/kg), anastrozole (4.03mg/kg), or exemestane (0.16mg/kg). Tissues of interest were collected at 7 days post onset of treatment and processed for their respective phenotypes (transcriptomics, SERM/E2 quantification or histology).

RNA isolation

Hippocampus cells was directly homogenized in TRIzol® Reagent (Invitrogen, 15596026) using The Bullet Blender® and silicon beads. Chloroform was used to extract RNA from the homogenate at a volume ratio of 1:5 to that of the TRIzol® Reagent. Ethanol was then used to precipitate nucleic acids from the aqueous phase. RNA was further purified using PureLink™ RNA Mini Kit (Invitrogen™, 12183018A) following manufacturer's instructions. Purelink™ DNase (Invitrogen™, 12185010) was used to eliminate DNA contamination. Purified RNA was eluded in RNase-free, diH2O. RNA concentration and quality were checked by NanoDrop™ One UV-Vis Spectrophotometer (Thermo Fisher).

Real-time quantitative PCR assays

Gene expression of the 96 genes associated with estrogen pathways were determined using TaqMan® Array 96-well Human Estrogens Plates (ThermoScientific, 4413255) for the SH-SY5Y cells and TaqMan® Array Rat 96-well Estrogen Signaling Plates (ThermoScientific, 4413255) for the E18 rat hippocampal neurons. Briefly, RNA was converted to cDNA using SuperScript VILO cDNA Synthesis Kit (ThermoFisher, 11754050). A total of 6.25ng of cDNA was used per rt-PCR reaction along with TaqMan™ Universal PCR Master Mix (Applied Biosystems, 4304437). Target mRNA was amplified using the Applied Biosystems™ QuantStudio™ 12K Flex system. Relative gene expression level (fold change) to reference group was calculated by the comparative Ct ($\Delta\Delta$Ct) method. Statistical significance was calculated by ANOVA followed by non-paired t-test.

Bulk RNA sequencing (RNA-Seq)

RNA-Seq was conducted on hippocampal RNA at Vanderbilt Technologies for Advanced Genomics (VANTAGE). Only RNA samples with an acceptable RNA quality indicator score (RQI >7) were used for sequencing. Enrichment of mRNA and library preparation of cDNA were done using a stranded mRNA (poly(A) - selected) sample preparation kit. Sequencing was performed at 100bp paired-end on NovaSeq600, targeting 30 million reads per sample. The raw fastq sequencing data were mapped to rat cDNA library ensembl104 using salmon version 1.5.2[116] to get the expression counts of each transcript. DESeq2[117] and tximport[118] were applied to analyze the differentially expressed genes between different groups.

Ingenuity pathway analysis (IPA) of RNA-Seq and biological pathway analysis

Differentially expressed gene lists were processed using the core analysis function of IPA. To get robust analytical results, only genes with p-value smaller than 0.05 was considered. The outputs are lists of altered canonical pathways and upstream regulators. The canonical pathways are identified based on enrichment of qualified genes. The upstream regulator analysis predicted activation or inhibition of regulatory molecules based on expression of respective downstream genes and networks compiled from literature and IPA's Ingenuity knowledge base. Biological pathway analysis was conducted using Drug-Target Interaction (DTI) network approach. For each EMT identified, the related gene targets were extracted using DrugBank database.[24]

QUANTIFICATION AND STATISTICAL ANALYSIS

Medical informatics

Statistical analyses were conducted between January 1st and February 2nd, 2022. Patient demographic statistics and incidence statistics were analyzed using unpaired 2-tailed t-tests or $\chi 2$ tests, as appropriate, to test the significance of the differences between continuous and categorical variables. In all analyses, a 2-sided $P < 0.05$ was considered statistically significant. A propensity score-matched population was generated by using a logistic regression to identify confounding factors for therapeutic treatment of T2D as outcome between the treatment and control groups as previously reported.[18,104]

General statistical analysis

The experiments were repeated at least three times, and the results are expressed as the means and the standard error of the mean (SEM). Student's t tests (two-tailed) and two-way analysis of variance (ANOVA) were used to compare the means of two or more samples unless otherwise indicated. The P-values for each analysis were adjusted using the Benjamini-Hochberg method for multiple-testing correction when necessary. The cumulative recurrence and survival rates were determined using the Kaplan-Meier method (log-rank test). All data was visualized in R using summary statistics and basic plotting functions before statistical testing, and variance was comparable in all cases in which the Wilcoxon rank-sum test was used. All reported P-values were two tailed, and differences were considered to be statistically significant when the P-value was less than 0.05.